



**British
Geological Survey**
Expert | Impartial | Innovative

Handheld X-Ray Fluorescence; a method for non-destructive compositional analysis of sandstone building stones

Minerals and Waste Programme
Internal Report OR/16/008

BRITISH GEOLOGICAL SURVEY

MINERALS AND WASTE PROGRAMME

INTERNAL REPORT OR/16/008

Handheld X-Ray Fluorescence; a method for non-destructive compositional analysis of sandstone building stones

P A Everett and M R Gillespie

Editor

S F Parry

Keywords

Non-destructive; sandstone; HH-XRF; compositional analysis.

Bibliographical reference

EVERETT, P. A. AND GILLESPIE, M. R. 2019. Handheld X-Ray Fluorescence; a method for non-destructive compositional analysis of sandstone building stones. *British Geological Survey Internal Report, OR/16/008*. 44pp.

Copyright in materials derived from the British Geological Survey's work is owned by UK Research and Innovation (UKRI) and/or the authority that commissioned the work. You may not copy or adapt this publication without first obtaining permission. Contact the BGS Intellectual Property Rights Section, British Geological Survey, Keyworth, e-mail ipr@bgs.ac.uk. You may quote extracts of a reasonable length without prior permission, provided a full acknowledgement is given of the source of the extract.

BRITISH GEOLOGICAL SURVEY

The full range of our publications is available from BGS shops at Nottingham, Edinburgh, London and Cardiff (Welsh publications only) see contact details below or shop online at www.geologyshop.com

The London Information Office also maintains a reference collection of BGS publications, including maps, for consultation.

We publish an annual catalogue of our maps and other publications; this catalogue is available online or from any of the BGS shops.

The British Geological Survey carries out the geological survey of Great Britain and Northern Ireland (the latter as an agency service for the government of Northern Ireland), and of the surrounding continental shelf, as well as basic research projects. It also undertakes programmes of technical aid in geology in developing countries.

The British Geological Survey is a component body of the Natural Environment Research Council.

British Geological Survey offices

**Environmental Science Centre, Keyworth, Nottingham
NG12 5GG**

Tel 0115 936 3100

BGS Central Enquiries Desk

Tel 0115 936 3143

email enquiries@bgs.ac.uk

BGS Sales

Tel 0115 936 3241

email sales@bgs.ac.uk

**The Lyell Centre, Research Avenue South, Edinburgh
EH14 4AP**

Tel 0131 667 1000

email scotsales@bgs.ac.uk

Natural History Museum, Cromwell Road, London SW7 5BD

Tel 020 7589 4090

Tel 020 7942 5344/45

email bgs london@bgs.ac.uk

**Cardiff University, Main Building, Park Place, Cardiff
CF10 3AT**

Tel 029 2167 4280

**Maclean Building, Crowmarsh Gifford, Wallingford
OX10 8BB**

Tel 01491 838800

**Geological Survey of Northern Ireland, Department of
Enterprise, Trade & Investment, Dundonald House, Upper
Newtownards Road, Ballymiscaw, Belfast, BT4 3SB**

Tel 01232 666595

www.bgs.ac.uk/gsni/

**Natural Environment Research Council, Polaris House,
North Star Avenue, Swindon SN2 1EU**

Tel 01793 411500

Fax 01793 411501

www.nerc.ac.uk

**UK Research and Innovation, Polaris House, Swindon
SN2 1FL**

Tel 01793 444000

www.ukri.org

Website www.bgs.ac.uk

Shop online at www.geologyshop.com

Acknowledgements

The authors would like to thank Dr Charles Gowing for the use of the Handheld X-Ray Fluorescence equipment, training in its operation and for his advice on aspects of methodology.

Contents

Acknowledgements	i
Contents	i
Summary	iii
1 Introduction	1
2 Background	3
2.1 Previous studies	3
2.2 Properties of sandstone that might influence analytical results.....	3
3 Materials and methods	4
3.1 The HH-XRF instrument	4
3.2 Test materials.....	5
3.3 Displaying and interpreting the data.....	8
4 The testing programme	9
4.1 Stage 1: Optimising sample analysis methodology and plotting parameters	9
4.2 Stage 2: Effect of sample surface condition	13
4.3 Stage 3: Effect of compositional maturity	16
4.4 Stage 4: Effect of stone texture.....	20
4.5 Stage 5: Differentiating samples of different provenance	26
5 Discussion and conclusions	30
5.1 Evaluation of experimental outcomes	30
5.2 Potential applications.....	31
5.3 Further work	32
6 References	33
Appendix 1: Details of samples, analyses and tests	34

FIGURES

Figure 1. Image showing the analysis of a large block of Blaxter sandstone.	5
Figure 2. Plotted results for up to 20 repeat analyses of a sample of Peakmoor sandstone (Peakmoor A).	11
Figure 3. Plotted results for up to 20 repeat analyses of a sample of Pennant sandstone (Pennant A).	12
Figure 4. Plotted results for sawn and broken sample surfaces	14
Figure 5. Plotted results for a sawn surface and a natural fracture surface in a sample of St Bees sandstone	15
Figure 6. Plotted results for wet and dry sample surfaces.....	15
Figure 7. Plotted results for four sandstones (three samples each) with varying compositional maturity (see text for details).....	19
Figure 8. Plotted results for a subset of samples with varying compositional maturity	19
Figure 9. Large block of Blaxter sandstone, marked with test locations	21
Figure 10. Plotted results of sandstone samples with varying grain size.....	23
Figure 11. Plotted results of Pitairlie siltstone samples analysed normal and parallel to bedding.....	24
Figure 12. Plotted results of analyses from a large block of Blaxter sandstone	25
Figure 13. Plotted results of analyses of multiple samples from the same quarry	26
Figure 14. Plotted results for three visually similar buff sandstones	27
Figure 15. Photographs of visually similar sandstones selected for testing.....	28
Figure 16. Plotted results for three visually similar orange sandstones	29

TABLES

Table 1. Summary details of samples selected for analysis	6
Table 2. Comparison of elements determined in analysed samples.....	18
Table 3. Average values and CV for key elements in selected samples.	18
Table 4. Details of samples and analyses	35
Table 5. Analyses in each stage of testing	36

Summary

This report describes a study designed to devise an appropriate methodology for using a Handheld X-Ray Fluorescence (HH-XRF) instrument for *in situ* testing of sandstone building stones. HH-XRF is a non-destructive method of compositional analysis that could offer the means to geochemically differentiate different sandstones, and constrain their quarry sources.

To examine the potential of HH-XRF for these purposes, a programme of laboratory tests has been conducted on a range of sandstone building stones from the UK. The aims of the test programme were to: develop and refine a robust and fit-for-purpose methodology for gathering, managing, displaying and interpreting compositional data; determine the extent to which sample surface condition and stone texture affect the results; and evaluate whether or not the results can provide a basis for distinguishing different sandstones.

The results suggest the instrument can be used to distinguish sandstones (and potentially a wide range of other geological and man-made materials) that are otherwise indistinguishable in the field, and as such the method should find widespread application in disciplines such as building conservation and archaeology.

1 Introduction

Sandstone is probably the most abundant and widely used building stone in the UK, both historically and currently. The geological diversity of the UK has resulted in a very wide range of sandstone building stones; several hundred different sandstones have been produced from several thousand quarries scattered widely across the country. This diversity, and the long history of sandstone use as a building material, has produced a very large and rich legacy of traditional sandstone buildings in the UK. For many years, BGS has supported the architectural conservation sector, typically by providing an applied geological understanding of the properties of building stones where this is needed to inform conservation issues.

Commonly, there is no written record of the source of the masonry in a traditional building, and a visual examination alone in many cases is inconclusive. In such situations, the provenance of the stone can only be constrained by distinguishing it from other stones on the basis of some distinctive property or characteristic, usually revealed by microscope examination or bulk chemical analysis of a detached sample. This can be of use for understanding the construction and repair history of a building, and it can help to identify (or constrain) stone provenance which might be helpful when selecting stone to use in building repairs. However, detaching samples from stone structures damages them, and analysing the stone by these conventional means can be difficult and time-consuming.

A means of non-destructively gathering compositional data from sandstone masonry could be of considerable benefit. Handheld X-Ray Fluorescence (HH-XRF) analysis is a non-destructive means of obtaining bulk composition data, which potentially offers the means to differentiate geological (and other) materials, and in some cases could help to constrain or confirm their provenance without the need to collect physical specimens.

X-Ray Fluorescence (XRF) spectrometry has been one of the principal means of analysing the chemical composition of rocks for many years. However, the size and sensitivity of the instruments, and the fact that they carry an X-Ray source, has meant that until recently XRF analysis has been confined to the laboratory. In recent years, handheld XRF instruments have been developed that are lightweight, wireless and fully portable. They provide a rapid, non-destructive means of analysing the composition of most inorganic materials, in a wide range of settings.

Sandstones from quarries in different lithostratigraphic units are likely to be derived from different source regions, and to have experienced different diagenetic histories. For these reasons, it is reasonable to expect that sandstones from different units will to some degree display distinctive bulk chemical compositions, even though they may be nearly identical in terms of appearance. HH-XRF analysis may provide the means to reveal differences in the compositional character of building stone sandstones without damaging the host structure.

Before this potential can be realised, the benefits and limitations of HH-XRF when applied to the testing of typical sandstone building stones need to be understood. The method is only likely to be considered useful, and to be adopted widely, if it is possible to obtain and evaluate a large number of analyses quickly and easily. In order to assess these criteria, the following objectives were defined for this study.

- To develop and refine a robust methodology for analysing sandstone building stones with an HH-XRF instrument.
- To develop a means of assessing and interpreting results quickly but with sufficient rigour to ensure they are meaningful.
- To determine the extent to which sample surface condition and stone texture affect the analytical results.

- To examine the extent to which sandstones from different sources can be discriminated using the analytical results.
- To evaluate the advantages, limitations and potential of the method for building stone applications.

To address these objectives, a five-stage programme of laboratory analysis has been carried out using samples from several sandstone quarries and an HH-XRF instrument.

Section 2 of this report provides background information, including a brief review of published studies that describe the application of HH-XRF to geological and other materials, and an overview of the typical properties of sandstone building stones that might be expected to influence the results.

Details of the instrument, test materials, and the approach used to display and interpret results throughout all stages of the test programme are presented in section 3. The objectives, results and outcomes for each stage of the test programme are described in section 4. A synthesis of the outcomes of the test programme, and the conclusions drawn from the study, are provided in section 5.

2 Background

2.1 PREVIOUS STUDIES

HH-XRF analysis has been applied successfully in several studies to determine the provenance of archaeological artefacts, for which non-destructive analytical methods are essential. In examples of this type of research, the analysed materials have included obsidian (Dyrdahl & Speakman, 2013; Cecil et al. 2007) and pottery (Morgenstein and Redmount, 2005) artefacts.

Most HH-XRF instruments are designed by the manufacturers to provide optimised analytical sensitivity for commodity elements and/or potentially harmful elements, (e.g. Pb, Zn, Cu), because the main customers are the mineral exploration industry and organisations working with contaminated land. HH-XRF analysis has been used chemostratigraphic applications in connection with borehole cores (oil and gas industry), rapid prospectivity analysis (mineral exploration industry; e.g. Fisher et.al. 2014) and contaminated land assessments.

The brief review of literature conducted at the inception of this study revealed only one example of HH-XRF analysis being applied to building stone (Historic Scotland, 2012); however, the details and outcomes of that work have not been published.

2.2 PROPERTIES OF SANDSTONE THAT MIGHT INFLUENCE ANALYTICAL RESULTS

Sandstone is a granular material that is typically porous and inhomogeneous (mineralogically and texturally). These properties present a considerable challenge for the effective application of HH-XRF analysis, as they have the potential to undermine the accuracy and precision of results.

The granular character of all sandstones, and the bedded (or laminated) character of many sandstones means they are anisotropic at a range of scales, which potentially makes it difficult to capture a set of analyses that adequately reflects the composition of an individual sample or the geological unit from which a sandstone was sourced. The relatively high porosity (up to c. 25%) of many sandstones also reduces the ability of the method to provide accurate quantitative analyses, unless a potentially complex and time-consuming data correction procedure, which accounts for the influence of porosity on accuracy, can be derived and proven to be effective.

Analysis of materials such as obsidian, ceramic, glass or slate would be expected to be more accurate and precise than analysis of sandstone, as they are comparatively homogenous and non-porous materials.

The surface conditions of analysed materials might also affect the quality of HH-XRF analysis. For example:

- *in situ* masonry and quarry exposures can be variably moist;
- masonry and sample surfaces can be variably weathered;
- masonry and sample surfaces can be flat and smooth (sawn) or irregular and rough (broken).

3 Materials and methods

3.1 THE HH-XRF INSTRUMENT

HH-XRF analyses were obtained using a Thermo Niton XLt 700 Series Environmental Analyser, which is referred to as the “the instrument” hereafter.

The instrument is simply pressed against the sample surface and ‘fired’ using a trigger (Figure 1). An X-ray beam produced by the source inside the instrument is absorbed by the sample. The analysed volume corresponds to an area approximately 8mm wide and up to 5mm deep. This produces a spectrum of secondary X-rays that are measured by the detector inside the instrument. The spectral response reflects the bulk chemical composition of the analysed volume.

The instrument is hand-held, and can be powered by mains supply or a re-chargeable battery pack. A shield is supplied, which fits onto the front end of the analyser to stop sample material from entering the instrument when testing loose matter, for example soil or sand.

An on-board CPU runs the instrument operating system; this allows the user to control some of the experimental parameters (such as ‘acquisition time’, i.e. the duration that the X-Ray source and detector are active for each individual analysis). The CPU also records the measured spectral data (results for up to 3000 analyses can be stored simultaneously), and reports element concentrations on-screen after deriving these values by computing them from the raw spectral data. Data can be downloaded easily via USB connection to a PC loaded with the Niton Data Transfer program. This program allows the user to view the spectra and presents the computed element concentration values in a MicroSoft Excel spreadsheet.

The instrument is capable of determining the concentration (in parts per million [ppm]) of 22 elements;

Sb, Sn, Cd, Ag, Sr, Rb, Pb, Se, As, Hg, Zn, Cu, Ni, Co, Fe, Mn, Cr, V, Ti, Sc, Ca, K.

However, the concentration of an element is only reported by the instrument if it exceeds the Lower Limit of Detection (LLD) for that element. The LLD is determined by the instrument for each individual analysis but is not recorded (i.e. the instrument reports the concentration of an element, or that it is below LLD, but does not record what the LLD value is). Broadly speaking, LLD values tend to be lower for elements with higher atomic numbers than they are for elements with lower atomic numbers. The LLD for each element can vary from test to test, as it is also partly dependent on the composition and textural properties of the analysed sample. Therefore, fixed LLD values for a particular HH-XRF instrument are not usually supplied by the manufacturer.

The instrument can operate in a number of different modes; the appropriate mode for a particular study will depend on the properties of the material and the elements of interest; for example, “thin sample mode” is optimised for samples <1mm thick, and “industrial bulk mode” is optimised for the commodity elements Cu, Zn and Pb. For this study, the instrument was run in “standard bulk mode” (optimised for soil testing), which offers balanced analytical sensitivity across the full range of measured elements and is designed for use when the elements of interest are present in low concentrations (<1% of the total sample).

A calibration routine, which is built-in to the CPU, was run before each analysis session. This measures the X-ray spectra and adjusts the internal electronics and sensors according to pre-loaded factory settings. This means that results should be internally consistent but may not be comparable with data produced using a different instrument.

Improved accuracy and standardised results might be achieved if a calibration routine using reference samples of known composition was adopted (as is employed for most forms of high-precision compositional analysis). However, such a procedure is beyond the scope of this study as the textural character and heterogeneity of conventional reference standards are drastically different from those of sandstone, rendering them unsuited to this application.

3.2 TEST MATERIALS

The programme of laboratory analysis was conducted on 24 hand samples (22 formed of sandstone, 2 of siltstone) sourced from quarries at 12 locations in the UK (Table 1). For brevity, these are referred to collectively as ‘sandstones’ in this report, while the stone from a single location is referred to using the quarry name and the term ‘sandstone’ (e.g. ‘Blaxter sandstone’).

The suite of samples is intended to encompass the typical range of mineral-textural and surface characteristics that might be encountered in UK buildings and samples of UK building stone, and includes:

- Sandstones with a range of colours, including the common orange, white and buff variants.
- Samples from a range of lithostratigraphic units that span various chronostratigraphic divisions.
- Samples with a range of grain size and textural characteristics.
- Samples featuring both rough and smooth surfaces.
- Samples that in mineralogical terms range from very mature (quartz-rich) to immature (with greater proportions of feldspar and lithic detrital grains).
- Samples of sandstone that are visually indistinguishable.
- Samples from multiple quarries in the same geological formation.

All the samples were obtained from the BGS Collection of UK Building Stones, and all consist of fresh (unweathered) stone.

Typical sandstone building stones are composed predominantly of detrital sand grains, formed principally of quartz, feldspar and rock fragments in varying proportions. A range of other minerals, including mica, Fe (-Ti) oxide, apatite, tourmaline and zircon, are usually present in minor to trace proportions. Secondary (authigenic) minerals, including calcite, dolomite, iron oxide (or oxyhydroxide), clay and quartz, are commonly present in minor to trace proportions. Most building stone sandstones are porous (up to 25% pore volume). The elemental concentrations measured by the instrument should be strongly controlled by the composition and relative proportions of the detrital grains in the sandstone. Quartz (SiO_2), which is usually the dominant constituent, produces no response from the instrument, as neither Si nor O are measureable elements, so the compositional maturity of a sandstone (i.e. the proportion of quartz relative to other detrital components) has the potential to influence the analytical results.

To examine how detrital grain composition influences the analytical results, average amounts of the principal detrital constituents and pore space in each sandstone were estimated by a visual examination of thin sections using an optical microscope and recorded as a percentage of the thin section area (Table 1). For the purposes of this study, the terms used to describe compositional maturity were based on the proportion of the thin section area occupied by quartz, as follows:

- ‘very mature’; >70% of the thin section is quartz
- ‘mature’; 50-70% quartz
- ‘moderately mature’; 40-50% quartz
- ‘immature’; <40% quartz.



Figure 1. Image showing the analysis of a large block of Blaxter sandstone.

Table 1. Summary details of samples selected for analysis

Sandstone name	Compositional maturity	Colour	Modal composition (visual estimate in thin section)	BGS sample number(s)	Lithostratigraphic and chronostratigraphic association
Craikleith	Very mature	White	72% Quartz <1% Rock fragments 3% Feldspar <1% Mica 0% Iron oxide 3% Clay 15% Pore space 7% Silica overgrowth	MC5705	Gullane Sandstone Formation, Strathclyde Group; Carboniferous
Cullalo	Very mature	White	78% Quartz <1% Lithic grains 4% Feldspar 0% Mica <1% Iron oxide <1% Clay 16% Pore space 2% Silica overgrowth	MC8233	Sandy Craig Formation, Strathclyde Group; Carboniferous
Blaxter	Mature	Buff	58% Quartz 2% Rock fragments 6% Feldspar 2% Mica 3% Iron oxide 10% Clay 15% Pore space 3% Silica overgrowth 4% Other	MC10297 MC7333 ED10488 ED10815	Tyne Limestone Formation; Carboniferous
Stanton Moor	Mature	Buff	59% Quartz 3% Rock fragments 15% Feldspar 1% Mica 2% Iron oxide 5% Clay 12% Pore space 1% Silica overgrowth 2% Other	MC8760	Ashover Grit, Millstone Grit Group; Carboniferous,
Peakmoor	Mature	Buff	55% Quartz 2% Rock fragments 14% Feldspar 2% Mica 4% Iron oxide 8% Clay 12% Pore space 2% Silica overgrowth 1% Other	MC8528 ED10806 MC12093	Ashover Grit, Millstone Grit Group; Carboniferous
Crosland Hill	Moderately mature	Buff	49% Quartz 8% Rock fragments 10% Feldspar 1% Mica 4% Iron oxide 14% Clay 8% Pore space 6% Silica overgrowth	MC8535 MC9559	Rough Rock, Rossendale Formation, Millstone Grit Group; Carboniferous

Sandstone name	Compositional maturity	Colour	Modal composition (visual estimate in thin section)	BGS sample number(s)	Lithostratigraphic and chronostratigraphic association
Swinton	Moderately mature	Buff	43% Quartz 10% Rock fragments 8% Feldspar 3% Mica 2% Iron oxide 7% Clay 20% Pore space 3% Silica overgrowth 4% Other	MC8228 ED10475 ED10591	Ballagan Formation, Inverclyde Group; Carboniferous
Corsehill	Moderately mature	Orange	48% Quartz 8% Rock fragments 5% Feldspar <1% Mica 10% Iron oxide <1% Clay 25% Pore space 3% Silica overgrowth 1% Other	MC5857	St Bees Sandstone Member, Chester Formation; Triassic
St Bees	Moderately mature	Orange	41% Quartz 12% Rock fragments 1% Feldspar <1% Mica 10% Iron oxide <1% Clay 27% Pore space 4% Silica overgrowth 5% Other	ED110476 MC13070 ED10972	St Bees Sandstone Member, Chester Formation; Triassic
Cove	Moderately mature	Orange	47% Quartz 10% Rock Fragments 2% Feldspar 0% Mica 15% Iron oxide <1% Clay 18% Pore space 5% Silica overgrowth 3% Other	MC8527	St Bees Sandstone Member, Chester Formation; Triassic
Pennant	Immature	Purplish grey	30% Quartz 45% Rock fragments 2% Feldspar <1% Mica 0% Iron oxide 12% Clay 7% Pore space 1% Silica overgrowth 2% Other	MC8372 - 4	Pennant Sandstone Formation; Carboniferous
Pitairlie	Immature	Bluish grey	34% Quartz 20% Rock fragments 15% Feldspar 7% Mica 4% Iron oxide 3% Chlorite 1% Clay 7% Pore space 3% Silica overgrowth	MC11363 (sandstone) MC8685 MC11361 (siltstone)	Dundee Flagstone Formation; Devonian

3.3 DISPLAYING AND INTERPRETING THE DATA

A key objective of this study was to develop a means of gathering, assessing and interpreting analytical results quickly but with sufficient rigour to ensure they are meaningful. This is important because the method is only likely to be widely adopted if it is quick and easy to use, without the need for the data manipulation and rigorous statistical evaluation that is often employed in studies using bulk composition data. Ideally, a single set of elements or element ratios would be used to represent sandstone compositions, and the data would be evaluated using a simple, empirical method. With these objectives in mind, X-Y scatterplots have been used as the basis for presenting and interpreting the results of this study. A spatial grouping of plotted points from a single sample is referred to as a “cluster”, and a simple visual assessment of cluster patterns has been used to judge the extent to which each sample (or each sandstone) is compositionally distinct. A statistical evaluation of the results has not been carried out, and the standard or experimental error involved with each analysis has not been taken into account.

4 The testing programme

The testing programme was conducted in five stages. In each stage, the results from a number of tests were used to address specific questions. The questions posed, the test methods, and the results and outcomes for each stage are described separately and in sequence in this section of the report. The outcomes of the first two stages of testing influenced the methods used in subsequent stages.

A scheme of alphanumeric codes was devised to label the analytical data for each test, which allowed the identity of each sample and repeat analysis to be classified in a shorthand form. Before each test, the appropriate code was entered via the instrument's control panel. The on-board CPU logs this code against the stored result of each analysis, and it is exported automatically as an identifier for each XRF spectrum and row in the data spreadsheet when these are downloaded. This allowed sub-sets of the data to be easily extracted and collated for plotting results. A table detailing the tests and samples that the scheme of codes refers to is provided in Appendix 1.

In many cases, analyses from one sample were used during more than one stage of testing; a table (Table 5) listing which analyses were taken into consideration during each stage of testing is presented in Appendix 1. The test data are provided in full in a spreadsheet of supplementary data that accompanies this report; the same scheme of analysis identifier codes is used in that spreadsheet.

Unless otherwise noted, multiple analyses of each sample were made at different, randomly distributed positions on its surface, in an effort to represent the compositional range of the stone at hand sample-scale.

4.1 STAGE 1: OPTIMISING SAMPLE ANALYSIS METHODOLOGY AND PLOTTING PARAMETERS

This stage was designed to optimise some aspects of the analytical methodology, and to identify the most useful elements to use in scatterplots.

4.1.1 Objectives

The following questions were addressed.

- What is the optimum data-acquisition time for each analysis?
- Which plotting parameters should be used for binary scatterplots?
- What is the optimum number of analyses per sample?

4.1.2 Methods

Three samples of texturally uniform sandstone that vary considerably in terms of compositional maturity – Pennant sandstone (immature), Peakmoor sandstone (mature) and Craigleith sandstone (very mature) – were selected for testing, to ensure the outcomes of this stage apply to most UK sandstones.

The following approach was used.

- Tests of 30 seconds and 60 seconds duration were performed on each sample to determine whether longer-duration tests produce a significant benefit in terms of data quality.
- Each sample was analysed 20 times to determine which elements are present in sufficient concentration to be useful.
- Different combinations of elements and element ratios were plotted to determine which plotting parameters would be most useful.

- The minimum number of repeat analyses needed to adequately represent the composition of a sandstone was determined by comparing plots displaying different numbers of repeat analyses.

Each analysis was obtained from a dry, sawn surface, to limit any effect that varying sample surface condition may have on results.

4.1.3 Results and outcomes

What is the optimum data-acquisition time for each analysis?

Longer acquisition times in theory should improve the quality of results. However, holding the instrument still with the trigger down for 60 seconds proved to be extremely difficult, and a set of analyses representing 60-second data-acquisition times therefore was not obtained. Long test times could be achieved by attaching the instrument to a lab stand, but such a system could not be used in field situations. Consequently, 30 seconds (which is achievable when the instrument is hand-held in the field) was adopted as the optimum data-acquisition time, which is considered fit-for-purpose.

Which plotting parameters should be used for binary scatterplots?

Of the 22 elements that were analysed for, only Fe, Ti, and K were present in concentrations consistently above the LLD in all 20 repeat analyses of all three sandstone samples. Sr and Rb concentrations also were consistently above the LLD in all analyses of the Peakmoor and Pennant sandstones, but were consistently below the LLD in the Craigleith sandstone.

The concentrations of these five elements in sandstones are controlled by many of the most important detrital and authigenic components, including: feldspars, rock fragments, micas and clay (K, Sr and Rb); ilmenite, magnetite and other 'heavy minerals' (Fe and Ti); carbonate minerals (Fe and Sr); and iron oxide minerals (Fe).

Using two-element ratios of geologically correlated elements (instead of single element concentrations) is deemed to greatly reduce the 'scattering' effect of some sources of primary heterogeneity (e.g. compositional layering) and secondary processes such as weathering.

With these factors in mind, Fe/Ti and Sr/Rb were used as the plotting parameters on all scatterplots.

Very low proportions of feldspar and rock fragments in the very mature Craigleith sandstone almost certainly explain why Sr and Rb are below the LLD in this case. The chosen plotting parameters, which include Sr/Rb, therefore are not well suited to Craigleith sandstone and other very mature sandstones, and another means of discriminating these sandstones will be required.

What is the optimum number of analyses per sample?

To assess how many analyses of a sample of uniform sandstone are typically required to define its compositional character on scatterplots, a series of plots representing between 4 and 20 repeat analyses of the Peakmoor and Pennant sandstones was prepared (Figure 2 and Figure 3). The results from the Craigleith sample were not plotted or used for this stage of the study since Sr and Rb concentrations were below the LLD.

Both sandstones produced a similar result: on the X-Y plot, the data points form a well-defined cluster that expands up to around 10 analyses, but does not grow significantly thereafter (Figure 2 and Figure 3). On this basis, it is concluded that a minimum of 10 repeat analyses are required to represent the composition of a typical sample adequately. Therefore, for subsequent stages of the test programme, 10 repeat analyses were made to represent the composition of each sample. The size (and shape) of the data fields produced in this way represent the natural compositional variability of a sandstone on the hand sample-scale.

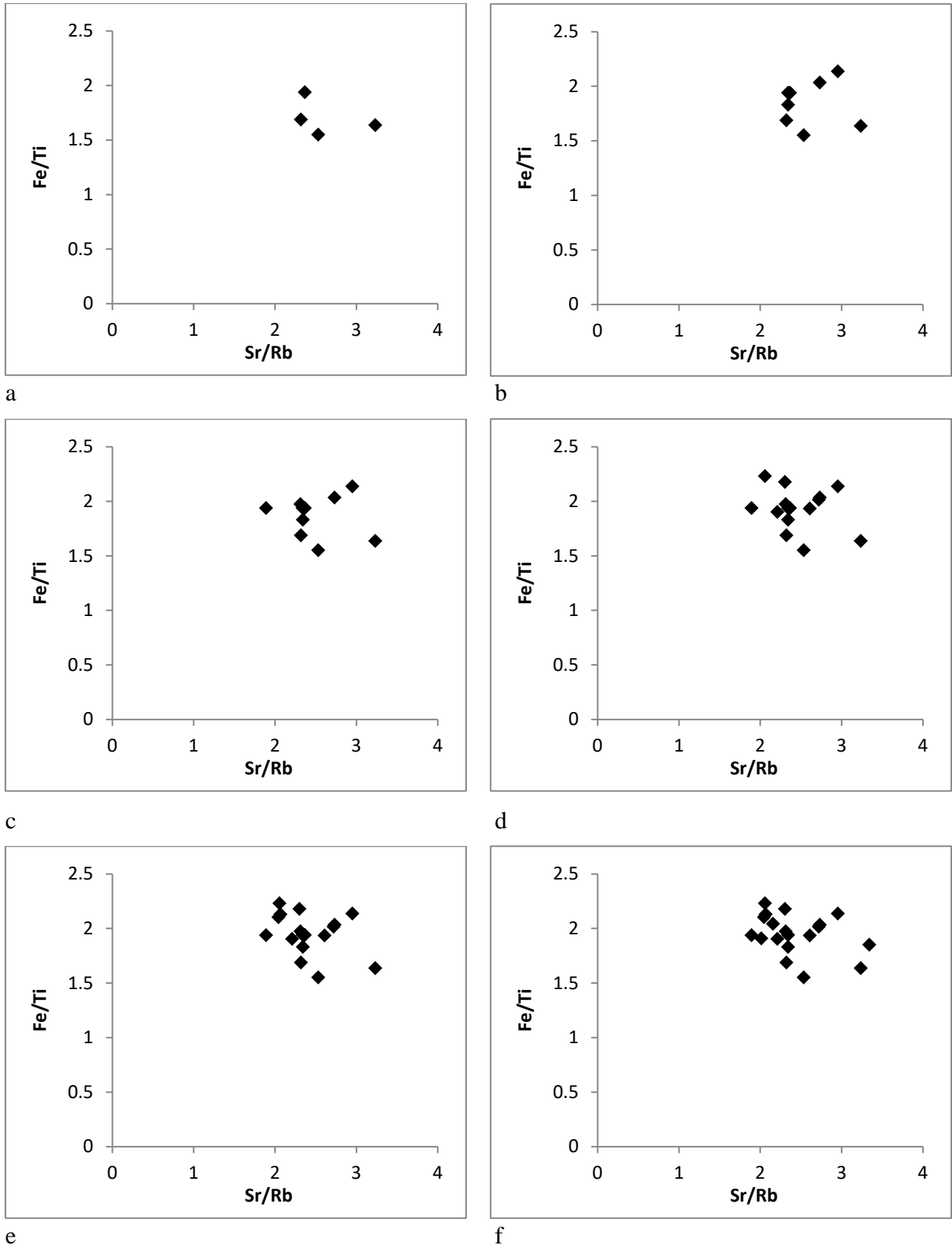
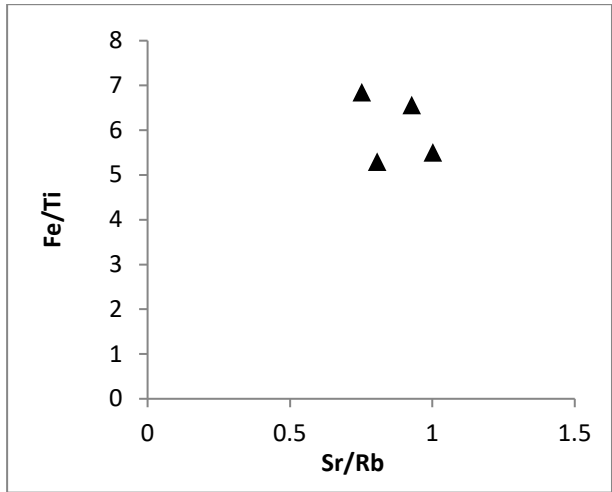
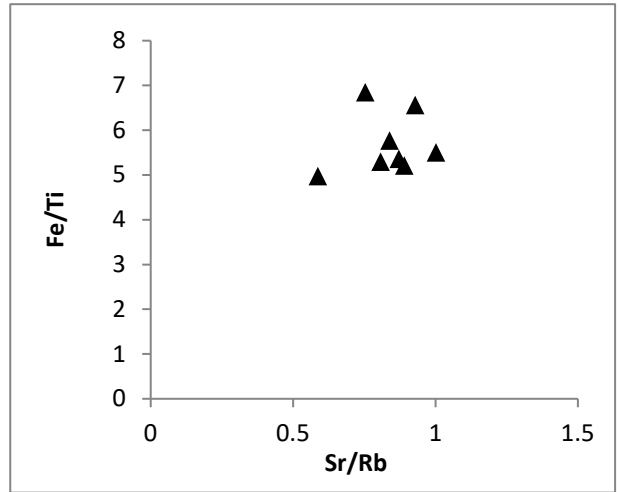


Figure 2. Plotted results for up to 20 repeat analyses of a sample of Peakmoor sandstone (Peakmoor A).

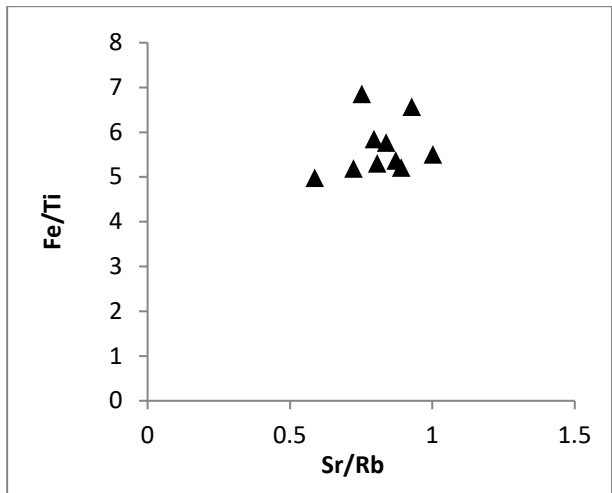
a – plot based on 4 analyses. b – plot based on 8 analyses. c – plot based on 10 analyses. d – plot based on 15 analyses. e – plot based on 17 analyses. f – plot based on 20 analyses.



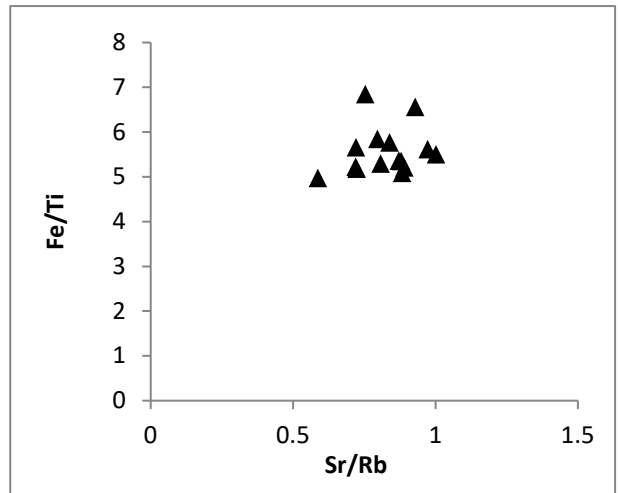
a



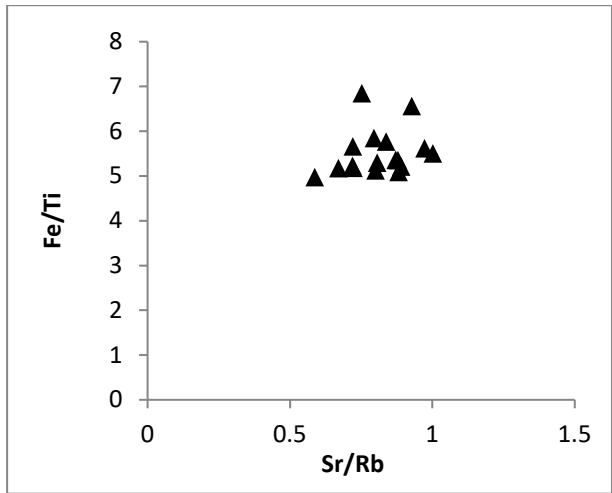
b



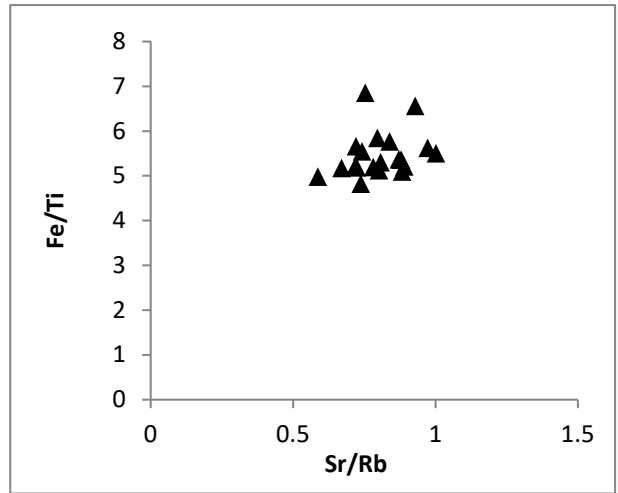
c



d



e



f

Figure 3. Plotted results for up to 20 repeat analyses of a sample of Pennant sandstone (Pennant A).

a – plot based on 4 analyses. b – plot based on 8 analyses. c – plot based on 10 analyses. d – plot based on 15 analyses. e – plot based on 17 analyses. f – plot based on 20 analyses.

4.2 STAGE 2: EFFECT OF SAMPLE SURFACE CONDITION

Sandstone building stones might be analysed in a range of settings, for example in the laboratory, in a quarry, and within masonry. The purpose of this stage was to examine how some common sample surface conditions encountered in these settings may affect the analytical results.

4.2.1 Objectives

The following questions were addressed:

- Does sample surface roughness have a significant effect on results?
- Does sample surface moisture (i.e. a wet or dry surface) have a significant effect on results?

4.2.2 Methods

- Six samples, each representing a different sandstone (Pennant, Pitairlie, Corsehill, Stanton Moor, Swinton and St Bees), and each featuring flat and rough surfaces, were tested to assess the effect of surface roughness. For each sample, ten analyses were made on a flat surface created with a diamond-blade saw, and ten were made on a freshly broken, rough surface. The sawn surfaces were cleaned to ensure pores were not blocked by rock powder from sawing.
- The surface of a natural fracture in the St Bees sandstone sample, which developed prior to quarrying, was also analysed ten times to allow a comparison with the freshly broken surface.
- Four samples representing different sandstones (Peakmoor, Craigleith, Corsehill, Pennant), were tested to assess the effect of surface moisture. In each case, ten analyses were made on a dry, flat surface, and ten more were made on the same surface after it was wetted with distilled water. Water was allowed to soak into the sample before the surface was analysed.

4.2.3 Results and outcomes

Does sample surface roughness have a significant effect on results?

For all six samples, the clusters defined by the analyses of the broken and sawn surfaces overlap to a considerable degree (Figure 4). The lack of any systematic difference indicates the small variations can be attributed mainly to minor, sample-scale, natural variation in bulk composition, and suggests that sample surface character has no significant impact on results. However, the distance and angle between the tested surface and the instrument's detector/X-Ray source will vary in a set of analyses made on a rough surface, so it seems sensible to restrict analyses to flat (sawn) surfaces wherever possible; only flat sample surfaces were used in subsequent stages of testing.

Analyses of a natural fracture surface and a freshly broken (man-made) surface of the St Bees sandstone sample form distinct (non-overlapping) clusters, due to consistently lower Fe concentrations on the man-made fracture surface (Figure 5). This can almost certainly be attributed to chemical alteration of wall rocks by fluids that migrated along the natural fracture, causing Fe (and Ca; see results in Appendix 2) to be leached and redistributed. We conclude therefore that naturally fractured surfaces should be avoided, even if they look similar to the rest of the sample, as they may be altered.

Does moisture (i.e. a wet surface) have a significant effect on results?

For all three samples, the clusters defined by analyses of the wet and dry surfaces overlap to a considerable degree (Figure 6). The lack of any systematic difference suggests the small variations can be attributed mainly to minor, sample-scale, natural variation in bulk composition, and suggests that sample surface wetness has no significant impact on the results. It should thus be possible to meaningfully compare results obtained from surfaces with a range of surface moisture conditions in real-world settings, but to maximise consistency it is probably sensible to test only dry surfaces where possible. Accordingly, dry surfaces were used in subsequent stages of testing.

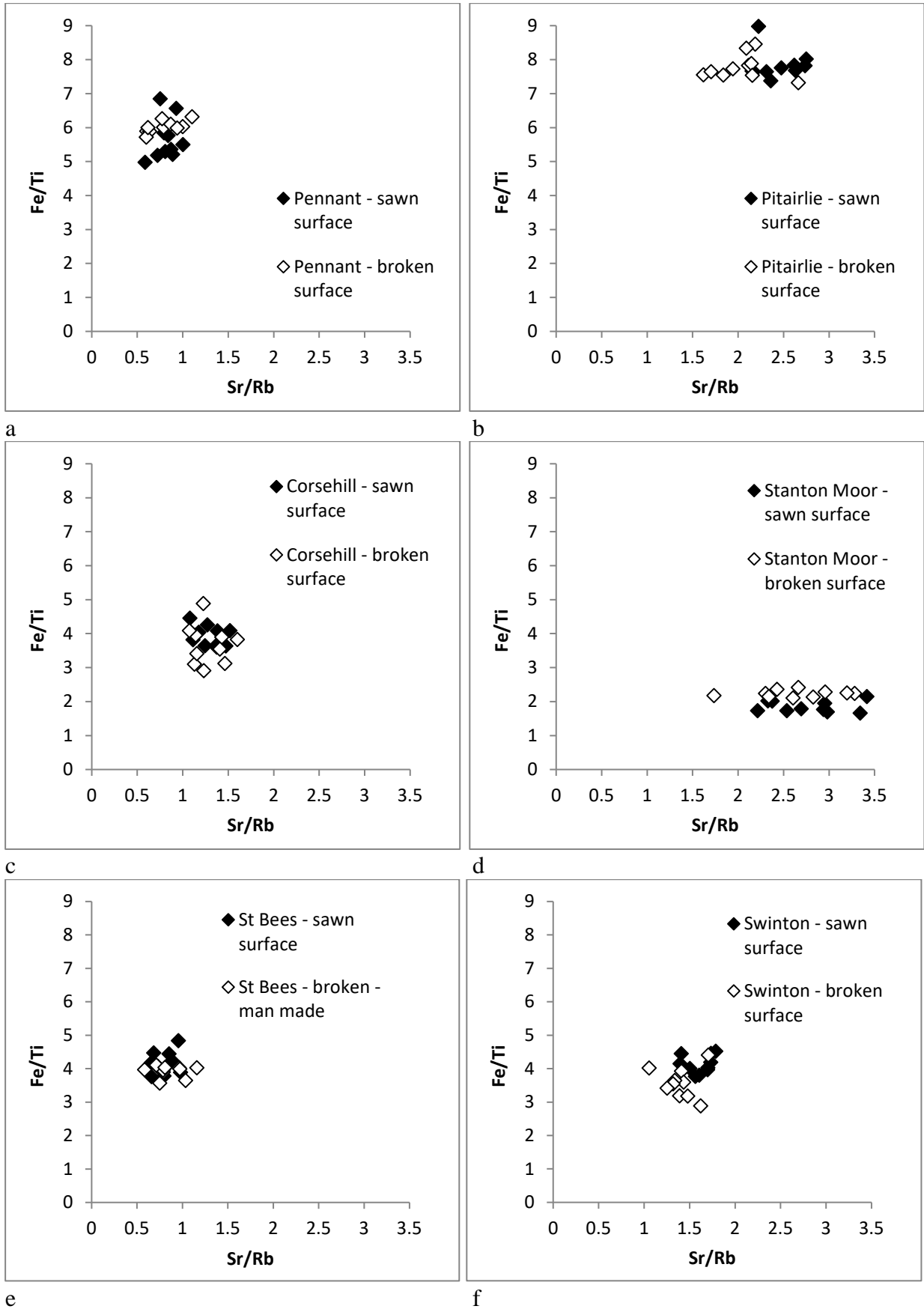


Figure 4. Plotted results for sawn and broken sample surfaces

Each plot compares the results from the sawn and broken surfaces of each of the six tested samples: a – Pennant. b – Pitairlie. c – Corsehill. d – Stanton Moor. e – St Bees. f – Swinton.

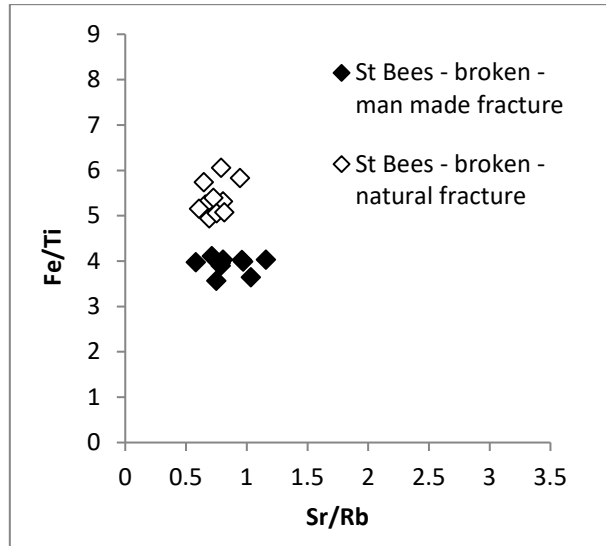


Figure 5. Plotted results for a sawn surface and a natural fracture surface in a sample of St Bees sandstone

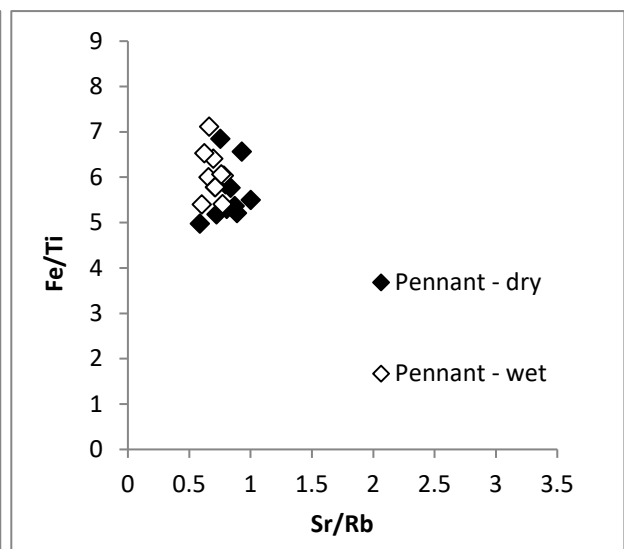
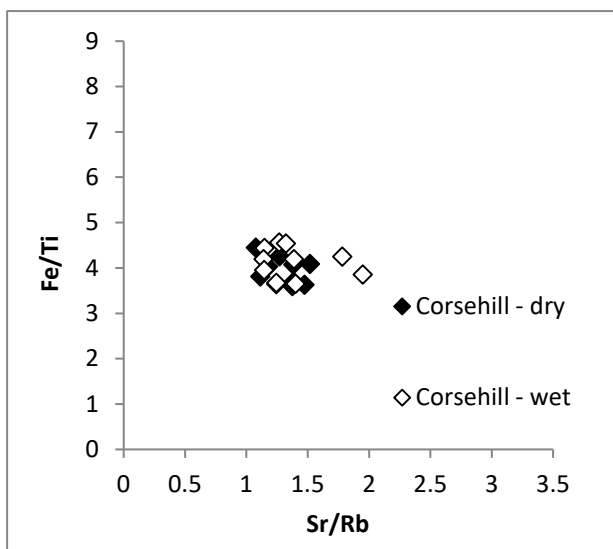
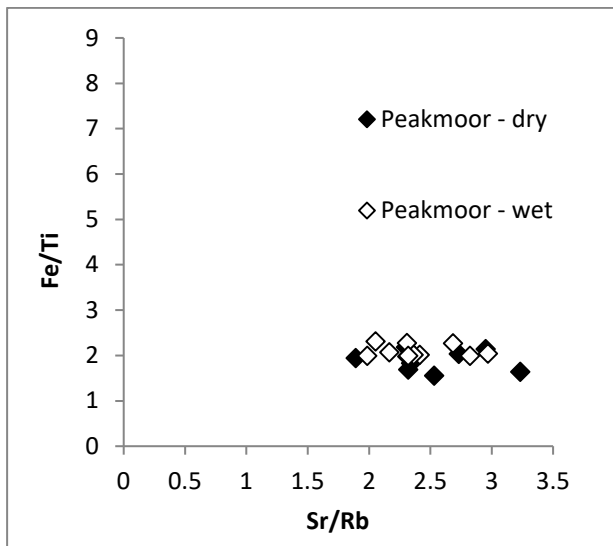


Figure 6. Plotted results for wet and dry sample surfaces

Each plot compares the results from the wet and dry surfaces of each of the three tested samples: a – Peakmoor. b – Corsehill. c – Pennant.

4.3 STAGE 3: EFFECT OF COMPOSITIONAL MATURITY

The compositional maturity of a sandstone, and the relative proportions of the main granular constituents (quartz, feldspar and lithic grains), should have a significant influence on the range and concentrations of elements determined by the instrument. The purpose of this stage of testing was to evaluate (in more detail than was described in section 3.2) the effect of compositional maturity on the reliability and utility of HH-XRF testing, and to verify the suitability of the plotting parameters identified in section 4.1.3.

4.3.1 Objectives

The following questions were addressed.

- How does the range of elements determined by the instrument (i.e. those above the LLD) vary in samples of different compositional maturity?
- How does the reliability of measurements for each element vary in samples of different compositional maturity?
- Can sandstones of different compositional maturity be distinguished by the HH-XRF method?
- How suitable are the selected plotting parameters for sandstones of different compositional maturity?

4.3.2 Methods

21 hand samples representing 12 UK sandstones were analysed. The selected samples are mineralogically and texturally uniform (not obviously bedded or laminated when viewed at the hand sample-scale), and dominantly sand-grade arenites with a range of compositional maturity. Each sample was analysed 10 times on a flat, dry surface.

4.3.3 Results and outcomes

How does the range of element concentrations determined by the instrument vary for samples of different compositional maturity?

Most of the elements that the instrument is capable of measuring (see section 3.1) were not determined in any of the samples (Table 2). The most frequently determined elements were Sr, Rb, Fe, Ti, and K, which were consistently above the LLD in all samples of mature, moderately mature and immature sandstone. The range of determined elements is much the same across this range of compositional maturity.

Rb was not consistently above the LLD in the analyses of the two very mature, quartz rich-sandstones (Craigeith and Cullalo). Sr was consistently above LLD in the Cullalo sample, but not in the Craigeith sample. Sub-LLD concentrations of these two elements are attributed to low proportions of feldspar and lithic grains in these very mature sandstones.

Ca was above LLD in the analyses of every sample of the Cove, St Bees, Stanton Moor and Pitairlie sandstones. Ca-rich minerals were not observed in thin sections of these samples, so they are not believed to be consistently present in significant volumes. Vanadium was consistently above LLD in all analyses of the Cullalo sample, but was not detected in any of the other sandstones.

Some other elements, most commonly Sn and Sb, but also As, Co, Mn, Cu and Cd, were above LLD in some samples but not in every repeat analysis.

How does the reliability of measurements for each element vary in samples of different compositional maturity?

Mean values and coefficient of variance (CV) values for the most commonly determined elements (Sr, Rb, Fe, Ti, and K) are presented in Table 2. Not surprisingly, the mean concentrations of these elements generally increase, and CV values correspondingly decrease, as compositional maturity decreases (Table 3).

A sub-set of the analyses for the Peakmoor, Blaxter, St Bees, and Swinton sandstones (three samples in each case) is plotted in Figure 7. The data for two of the Blaxter samples (A and B) display a much bigger range of Sr/Rb values than the other samples, and do not form tight clusters. Blaxter sandstone is compositionally mature, and the Sr and Rb data have the highest CV values of any sandstone analysed in this study; this means that much of the range in Sr/Rb values is probably due to poor analytical reproducibility (due to low element concentrations) rather than natural compositional variation. The data for Blaxter sandstone, therefore, are considered unreliable. This result highlights the importance of taking into account CV values at an early stage, particularly for analyses of multiple samples of compositionally mature sandstones that do not produce tight clusters on scatterplots.

For the three remaining sandstones (Peakmoor, St Bees and Swinton):

- The data for individual samples typically form tight clusters, demonstrating that the instrument is capable of producing results that can be used to characterise and distinguish sandstones on an empirical basis.
- Data clusters for different samples of the same sandstone sometimes overlap on the scatterplot and sometimes do not; this probably reflects differences in the degree to which sandstones display real compositional variation on the bed or quarry scale.
- The data for all samples of a single sandstone define a well-constrained and largely distinct field; each field represents a compositional ‘fingerprint’ for the sandstone.

Can sandstones of different compositional maturity be distinguished by the HH-XRF method?

Results for one sample of each sandstone (other than Blaxter, which is omitted as the data are considered unreliable; see above) are plotted on Figure 8. Samples representing different categories of maturity produce data clusters that lie in different regions of the scatterplot, allowing them to be distinguished quite readily. The Fe/Ti ratio is the main factor distinguishing the clusters: Fe/Ti values increase as compositional maturity decreases.

How suitable are the selected plotting parameters for sandstones of different compositional maturity?

In samples of very mature sandstone, only K, Fe and Ti were measured in concentrations above the LLD. This finding confirms that the plotting parameters selected for use here (which include Sr/Rb) are not suitable for discriminating very mature sandstones.

Sr, Rb, Fe, Ti, and K are the most consistently and reliably determined elements in analyses of mature, moderately mature and immature sandstones. This result confirms that these elements are the most suitable for distinguishing and comparing sandstone building stones using HH-XRF analysis (and the instrument used here), and the selected plotting parameters (Fe/Ti vs Sr/Rb) therefore are probably the best available. However, it will be important to consider the analytical reproducibility (i.e. CV values) of mature sandstones, to evaluate whether the data are reliable.

Table 2. Comparison of elements determined in analysed samples

Sandstone	Compositional maturity	Elements determined in every test	Elements determined in some tests	Elements that were not determined in any tests
Craigleith	Very mature	Fe, Ti, K	Sb, Sn, Cd, Sr, As	Ag, Rb, Pb, Se, Hg, Zn, Cu, Ni, Co, Mn, Cr, V, Sc
Cullalo	Very mature	Sr, Fe, V, Ti, K	Sb, Sn, Rb	Cd, Ag, Pb, Se, As, Hg, Zn, Cu, Ni, Co, Mn, Cr, Sc, Ca
Blaxter	Mature	Sr, Rb, Fe, Ti, K	Ca, Cu	Cd, Ag, Pb, Se, As, Hg, Zn, Ni, Co, Mn, Cr, V, Sc.
Stanton Moor	Mature	Sr, Rb, Fe, Ti, Ca, K	Sb, Sn, Cd, Mn, V	Ag, Pb, Se, As, Hg, Zn, Cu, Ni, Co, Cr, Sc,
Peakmoor	Mature	Sr, Rb, Fe, Ti, K	Sb, Ca, V, Mn	Sn, Cd, Ag, Pb, Se, As, Hg, Zn, Cu, Ni, Sc, Cr, Co
Crosland Hill	Moderately mature	Sr, Rb, Fe, Ti, K	Sb, Sn, Co, V, Ca	Cd, Ag Pb, Se, As, Hg, Zn, Cu, Ni, Mn, Cr, Sc,
Swinton	Moderately mature	Sr, Rb, Fe, Ti, K	Sb, Sn, V, Ca	Cd, Ag, Pb, Se, As, Hg, Zn, Cu, Ni, Co, Mn, Cr, Sc,
Corsehill	Moderately mature	Sr, Rb, Fe, Ti, K	Sb, Sn, Cd, Pb, V, Ca	Ag, Se, As, Hg, Zn, Cu, Ni, Co, Mn, Cr, Sc
Cove	Moderately mature	Sr, Rb, Fe, Ti, Ca, K	Sb, As, Co, Mn, V	Sn, Cd, Ag, Pb, Se, Hg, Zn, Cu, Ni, Cr, Sc
St Bees	Moderately mature	Sr, Rb, Fe, Ti, Ca, K	Sb, Sn, As, Mn, V,	Cd, Ag, Pb, Se, Hg, Zn, Cu, Ni, Co, Cr, Sc
Pennant	Immature	Sr, Rb, Fe, Ti, K	Sn, Zn, V, Ca	Sb, Cd, Ag, Pb, Se, As, Hg, Cu, Ni, Co, Mn, Cr, Sc
Pitairlie	Immature	Sr, Rb, Fe, Ti, Ca, K	Sb, Pb, Zn, Mn, V, Cr	Sn, Cd, Ag, Se, As, Hg, Cu, Ni, Co, Sc

Table 3. Average values and CV for key elements in selected samples.

Sample	Maturity	Sr		Rb		Fe		Ti		K	
		Mean ppm	CV %	Mean ppm	CV %	Mean ppm	CV %	Mean ppm	CV %	Mean ppm	CV %
Craigleith A	Very mature	*	*	*	*	417.5	18.3	307.5	14.2	1702.8	14.8
Cullalo A	Very mature	64.1	8.9	*	*	282.3	15.9	499.1	22.7	2009.2	14.9
Blaxter A	Mature	125.0	6.4	14.9	26.9	3807.9	5.5	1630.4	4.5	5719.1	6.4
Blaxter B	Mature	48.5	14.9	15.2	20.5	3063.8	3.4	668.4	5.7	6943.9	4.9
Blaxter C	Mature	31.5	13.5	22.1	24.0	5290.2	5.1	1927.0	4.3	7754.8	6.6
Peakmoor A	Mature	78.8	7.6	33.1	19.2	5706.3	5.6	2856.6	6.0	16076.6	8.1
Peakmoor B	Mature	91.5	6.9	33.6	15.4	4572.2	4.0	2419.6	3.7	17061.0	2.9
Peakmoor C	Mature	79.1	9.0	39.9	10.5	7431.8	5.5	2577.6	2.6	17222.6	3.0
S. Moor A	Mature	79.4	7.2	29.1	14.8	4073.8	6.3	2210.7	6.3	15685.9	2.8
C. Hill A	Mod mature	54.8	10.9	30.1	17.4	5504.3	3.7	1483.6	4.3	15320.9	3.2
C. Hill B	Mod mature	49.7	11.3	25.6	12.6	5097.9	3.5	1380.4	3.5	14301.2	5.2
Corsehill A	Mod mature	54.8	3.8	42.5	10.7	4175.5	5.9	1065.0	5.9	19556.7	2.3
Cove A	Mod mature	59.8	5.2	69.0	6.6	8374.6	4.6	1915.0	3.7	24959.1	2.3
St Bees A	Mod mature	65.4	8.2	82.1	10.6	8014.5	8.2	1931.9	11.6	28210.7	2.9
St Bees B	Mod mature	52.2	6.5	76.2	9.3	5639.5	3.0	1126.7	4.5	25578.3	2.1
St Bees C	Mod mature	62.9	6.5	84.8	8.5	8023.0	3.7	1137.5	5.4	29869.8	2.3
Swinton A	Mod mature	109.0	7.0	70.2	8.7	10787.2	4.1	2592.2	5.2	34044.3	3.0
Swinton B	Mod mature	100.7	9.3	63.0	9.7	4621.0	6.0	1847.3	3.3	30590.4	2.6
Swinton C	Mod mature	107.7	10.5	71.9	10.2	13514.4	4.4	2999.0	3.9	36958.6	1.9
Pennant A	Immature	43.2	15.2	53.1	11.8	13289.2	4.8	2428.4	6.0	21433.4	5.6
Pitairlie A	Immature	134.0	4.6	55.2	8.0	25580.4	3.5	3265.3	4.2	23956.9	4.4

* indicates value below LLD. Coefficient of variation (CV) is a measure of the variation within a group of analyses; in this case, it is the standard deviation of 10 analyses divided by their mean, expressed as a percentage.

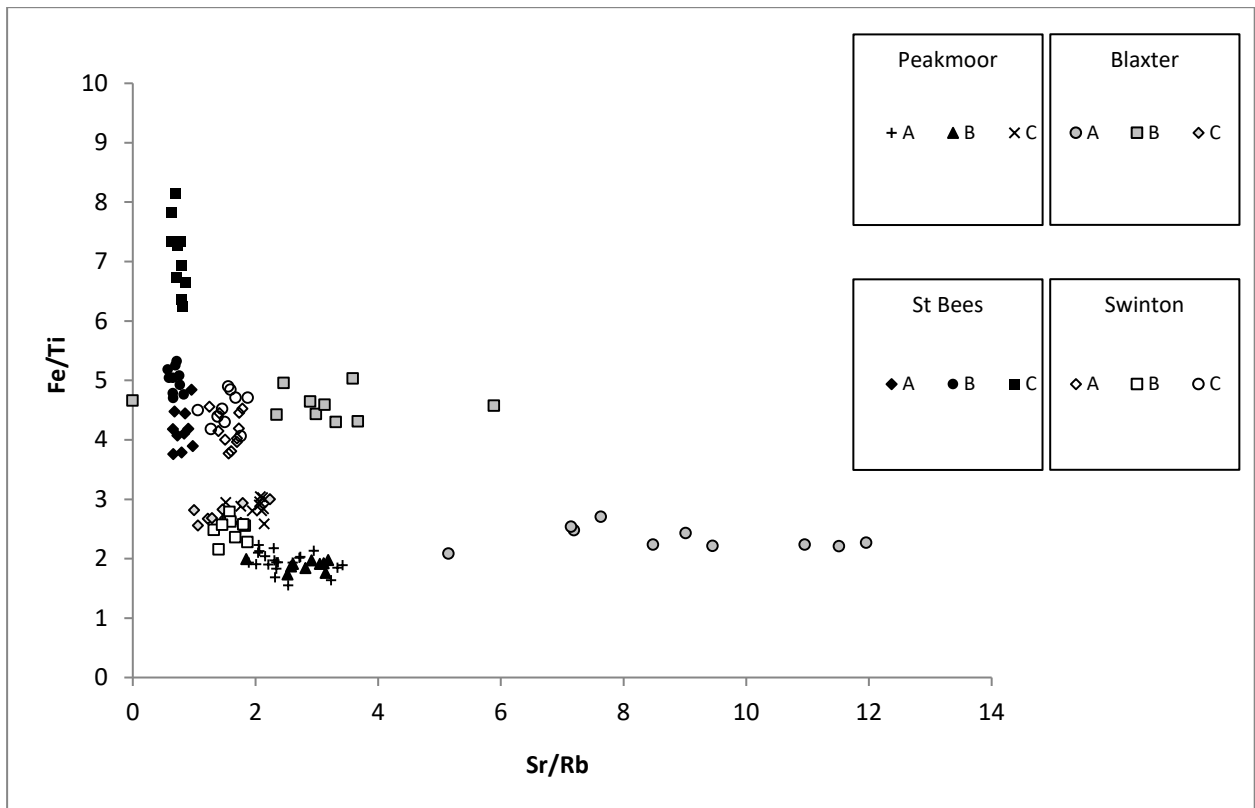


Figure 7. Plotted results for four sandstones (three samples each) with varying compositional maturity (see text for details)

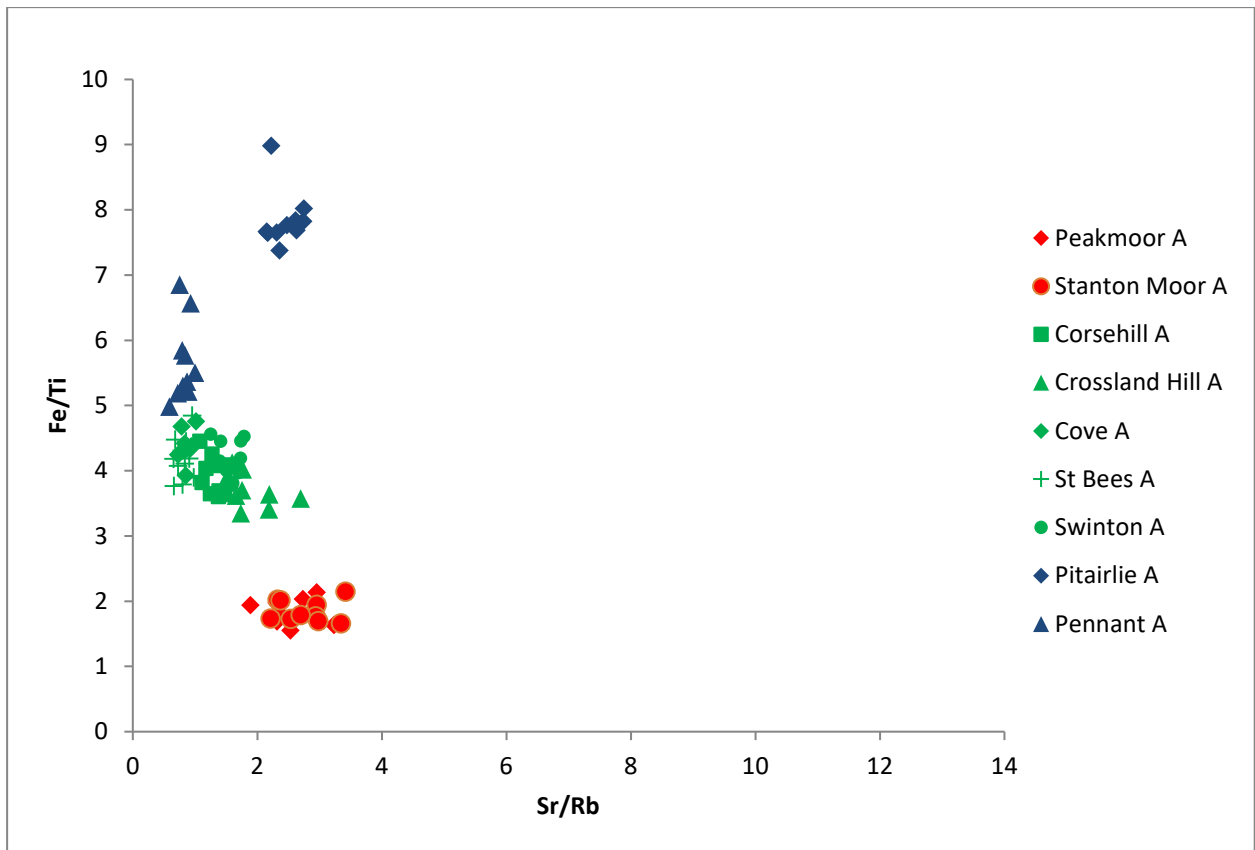


Figure 8. Plotted results for a subset of samples with varying compositional maturity

For clarity, the results from only one sample of each sandstone are plotted. Blue symbols represent immature sandstone, green symbols represent moderately mature sandstone, and red symbols represent mature sandstone.

4.4 STAGE 4: EFFECT OF STONE TEXTURE

This stage of testing was designed to assess the effect of grain size and textural variability on the HH-XRF results.

4.4.1 Objectives

The following questions were addressed:

- Does grain size have an effect on the consistency of results?
- Does bedding-related inhomogeneity (on the hand sample- to masonry block-scale) have a significant effect on results?

4.4.2 Methods

To examine the effect of grain size, samples of ‘fine’, ‘medium’, and ‘coarse’ sandstone from each of the Peakmoor, St Bees and Crosland Hill quarries were analysed. The terms ‘fine’, ‘medium’, and ‘coarse’ are used to distinguish relatively coarser and finer samples of the same sandstone; the terms do not imply an equivalent formal grain-size classification (for example, a sample described as ‘fine’ is not necessarily fine-grained according to the BGS grain-size scheme, but is finer than other samples from the same quarry).

To examine the effect of bedding-related inhomogeneity:

- Two samples of thinly bedded Pitairlie siltstone (Pitairlie B and C) were selected, and in each case ten analyses were spread across a single bedding plane (i.e. normal to bedding, testing a single bedding plane surface) and ten more were spread across (traversing) bedding (i.e. parallel to bedding, testing multiple bedding surfaces). The samples of Pitairlie stone are, strictly speaking, siltstone rather than sandstone, but they provide some of the best examples of thinly bedded siliciclastic building stones in the BGS collection.
- One large block (1.6m long and 0.5m wide) of Blaxter sandstone that lacks visible bedding features (the bedding orientation is only indicated by aligned mica flakes and mud clasts) was tested to determine whether bedding-related inhomogeneity could still be detected in visually ‘uniform’ sandstone. The block also displays brown and orange ‘liesegang bands’ that are approximately perpendicular to the inferred bedding orientation, so tests were also conducted to determine if any effect of this secondary alteration could be detected. The block has sawn surfaces and was tested in the following way (see Figure 9):
 - 12 x tests at “reference point 1” (red star)
 - 12 x tests at “reference point 2” (blue star)
 - 12 x tests traversing bedding (red triangles)
 - 12 x tests traversing liesegang bands (blue triangles)

Analyses for two other samples of Blaxter sandstone were shown to be unreliable in a previous stage of testing (see section 4.3.3). However, this block of Blaxter sandstone is the only sandstone sample in the BGS Collection of UK Building Stones that is large enough to allow analyses along traverse lines that cross both bedding and liesegang bands.

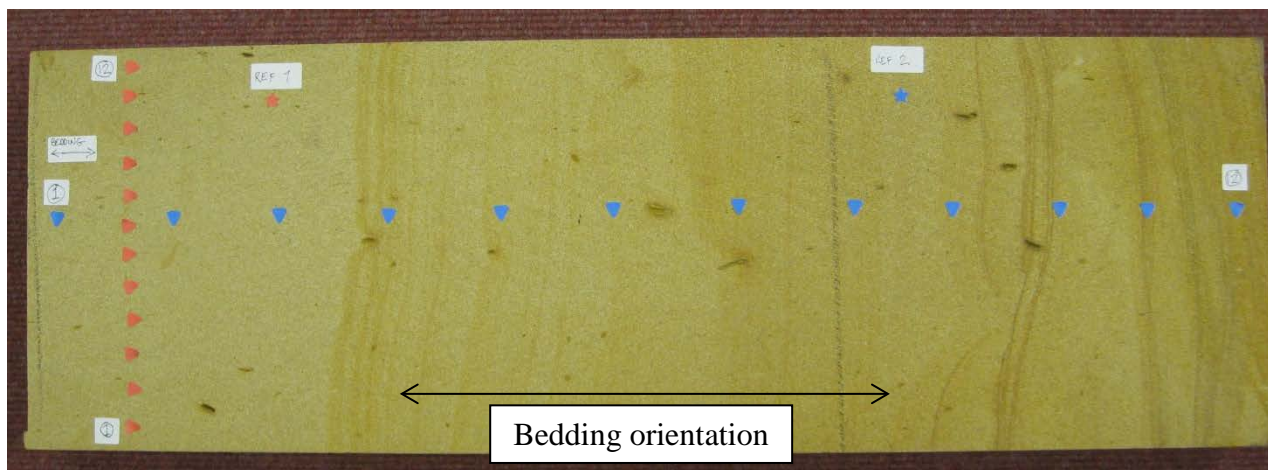


Figure 9. Large block of Blaxter sandstone, marked with test locations

The surface of the block is 1.6m x 0.5m in size. The orientation of the plane in which bedding intersects the block surface is shown; the obvious coloured bands at right angles to the bedding orientation are Liesegang bands. The surface was analysed along traverse lines both parallel and perpendicular to bedding: a single analysis was made at each location marked with a coloured triangle (red triangles are used for points traversing bedding, blue triangles for points traversing Liesegang bands). Twelve analyses were made at each of two ‘Reference points’ marked with a single coloured star (labelled REF1 and REF2).

4.4.3 Results and outcomes

Does grain size have an effect on the consistency of results?

The results from “fine”, “medium” and “coarse” samples of St Bees, Peakmoor and Crosland Hill sandstone are plotted in Figure 10. For each sandstone, clusters for the “fine”, “medium”, and “coarse” samples show a broadly similar size of spread. This suggests that grain size does not have a significant effect on the consistency of analyses, within the range of grain sizes typically exhibited by building stone sandstones. This interpretation makes sense since the maximum grain-size in any of these samples is around 1.5 mm, which is much smaller than the tested volume of each analysis (Section 2).

It is notable that the ‘fine’ Peakmoor and St Bees samples display higher Fe/Ti compared to the coarser samples of these stones. This may be related to a tendency for fine-grained sandstones to contain a greater proportion of Fe-bearing minerals, but this possibility cannot be properly evaluated on the basis of the limited number of samples analysed during this study.

Does bedding-related inhomogeneity have a significant effect on results?

Both samples of the thinly bedded Pitairlie siltstone (B and C; Figure 11) display subtly different but essentially similar ranges of Fe/Ti and Sr/Rb, indicating good overall consistency between samples and confirming that the mm-scale bedding variations in these samples have not had a significant effect on the results. In this case, the thinness of the bedding layers means that several layers will have been encompassed within the tested volume of any individual analysis made parallel to bedding, so any compositional variability in individual layers will have been ‘smoothed out’. Interestingly, analyses made normal to bedding and those made parallel to bedding cluster in different regions of the plot, with the latter consistently showing higher Sr/Rb. This may be because the low energy conditions under which siltstone is deposited allow platy flakes of mica to become relatively abundant in the stone and aligned with respect to bedding. This means they will comprise a larger proportion of the analysed volumes in measurements made normal to bedding than in those made parallel to bedding. Both main mica minerals – biotite and muscovite – are potassium-rich and therefore will have low Sr/Rb. Analyses made normal to bedding will therefore include a larger proportion of mica than those made parallel to bedding, so Sr/Rb will be lower.

The same compositional character would not be expected in most sandstones, because mica tends to be much less abundant and less strongly aligned.

Each of the two 'reference' locations in the block of Blaxter sandstone show well-constrained (tightly clustered) values, with essentially identical Sr/Rb at both locations and slightly higher Fe/Ti at reference location 2 (Figure 12). The small difference in Fe/Ti values is probably due to slightly different proportions of detrital Fe-Ti minerals and/or secondary Fe oxide/oxyhydroxide at this point. The traverse across bedding produced well-constrained (tightly clustered) values essentially identical to those made at reference location 1, confirming that any bedding-related inhomogeneity has had essentially no effect on the results. The traverse across liesegang bands produced the same range of Sr/Rb as at both reference locations, but a slightly broader range of Fe/Ti; the latter is almost certainly due mainly to slightly varying concentrations of secondary Fe oxide/oxyhydroxide produced by the same redox processes that created the liesegang bands. While this is an expected result, it is reassuring that the instrument has captured data that demonstrate variations due to secondary processes. This should be borne in mind when comparing sandstones with iron-related colour variations, as Fe may be an unreliable element for characterisation in this case. However, Ti, Sr, and Rb concentration data do not appear to be affected by the processes that produced the liesegang bands.

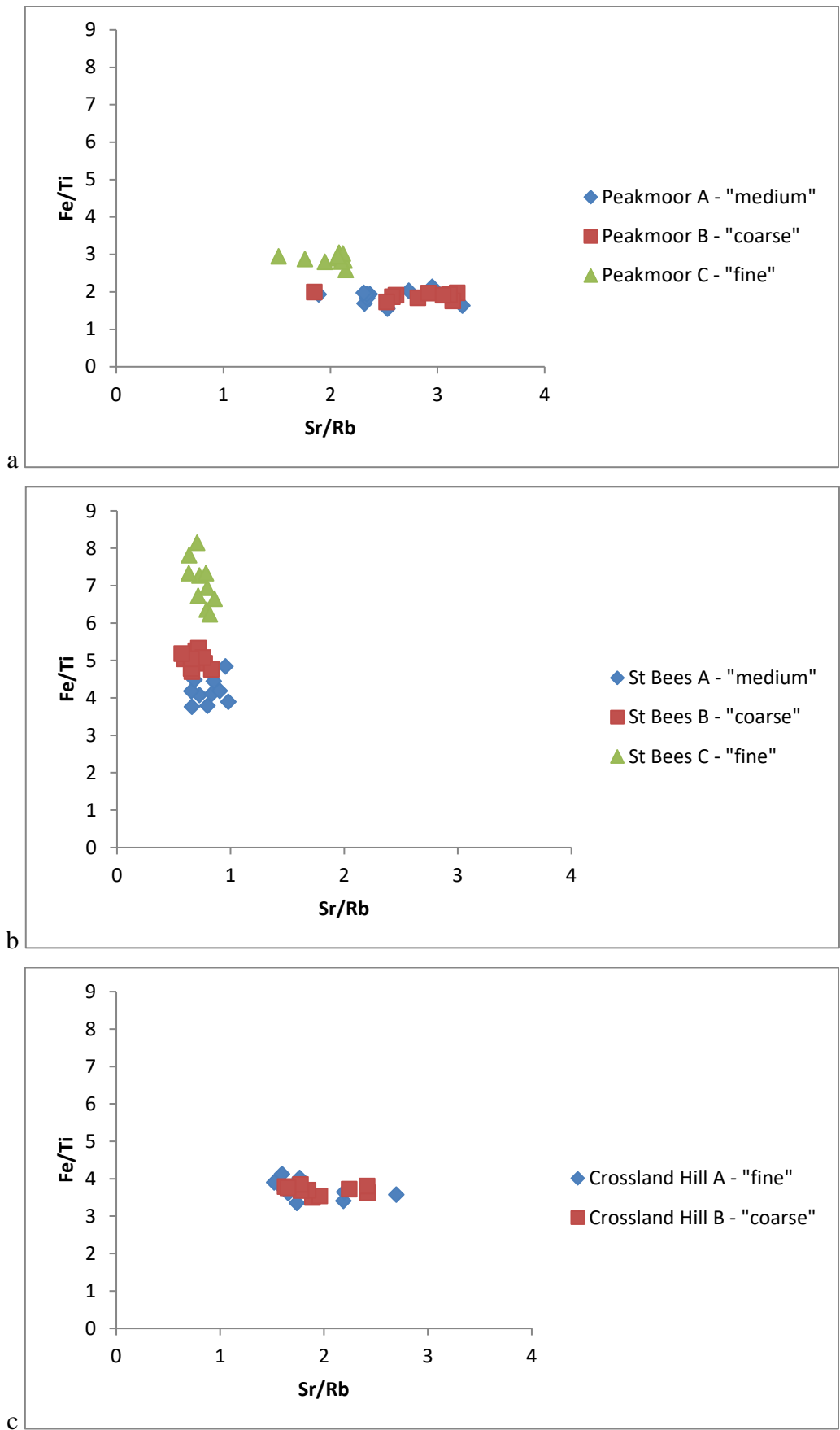


Figure 10. Plotted results of sandstone samples with varying grain size

a – Peakmoor. b – St Bees c – Crosland Hill

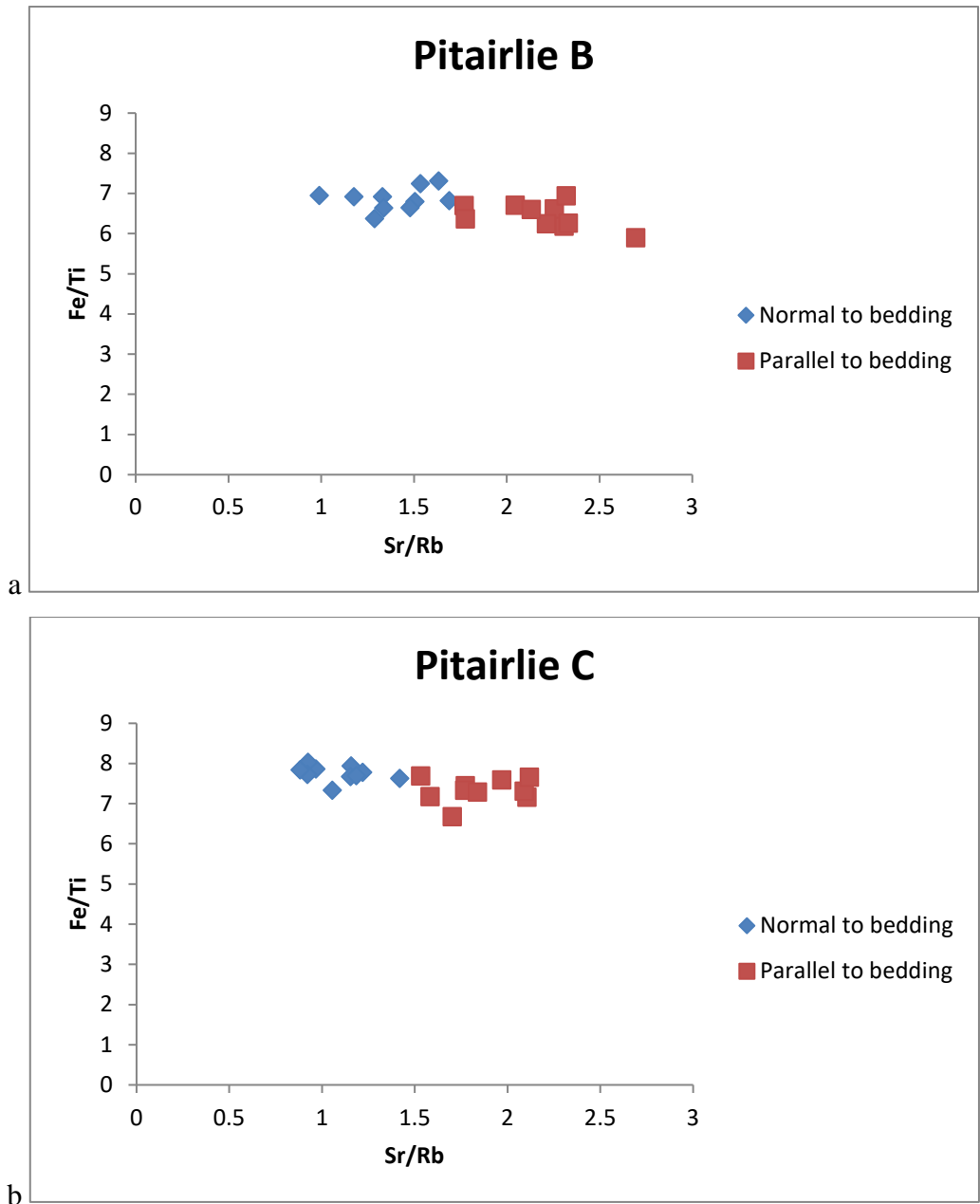


Figure 11. Plotted results of Pitairlie siltstone samples analysed normal and parallel to bedding

a – results from Pitairlie sample “B”. b – results from Pitairlie sample “C”

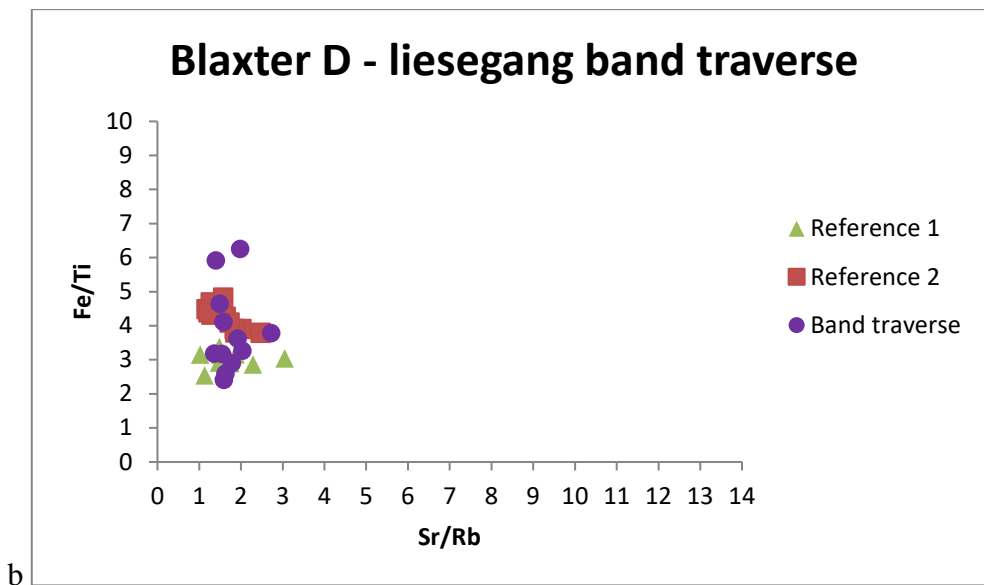
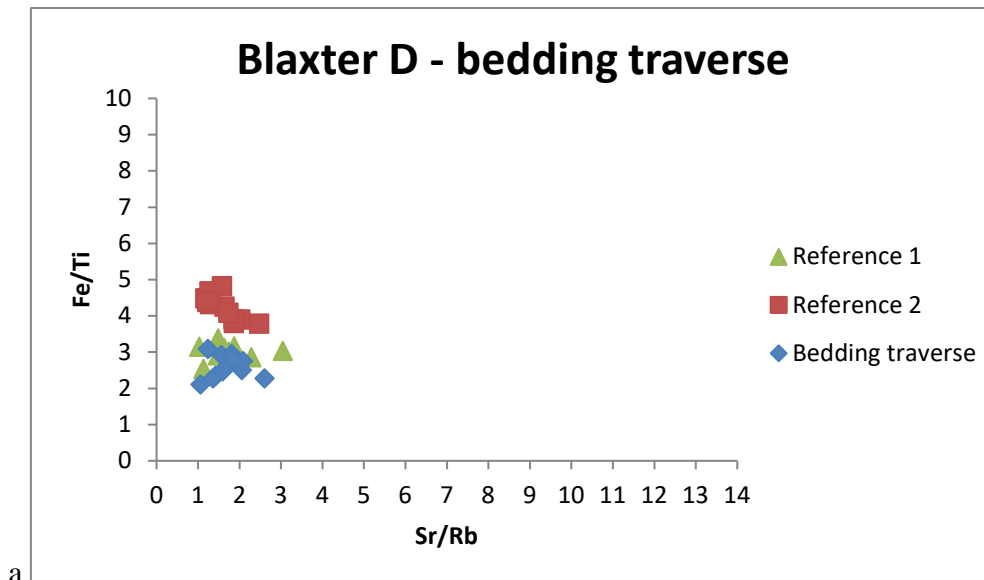


Figure 12. Plotted results of analyses from a large block of Blaxter sandstone

a – analyses collected from reference locations 1, 2, and a traverse normal to bedding. b – analyses collected from reference points 1, 2, and a traverse normal to liesegang bands.

4.5 STAGE 5: DIFFERENTIATING SAMPLES OF DIFFERENT PROVENANCE

4.5.1 Objectives

During the previous stages of testing, the optimum methodologies for analysing samples and plotting results have been established, and the effects of sample-scale factors other than provenance – including sample surface condition, varying compositional maturity, and varying stone texture – have been evaluated. In this final stage of testing, we aimed to address whether the HH-XRF instrument can differentiate sandstones of different provenance, in particular those that might otherwise be difficult to distinguish.

The tests used in this stage addressed the following questions:

- Can the method distinguish sandstones at the quarry scale and bedrock-unit scale?
- Can the method reliably distinguish sandstones that cannot be distinguished visually?

4.5.2 Methods, results and outcomes

Can the method distinguish sandstones at the quarry scale and bedrock-unit scale?

To assess whether the method can distinguish sandstones at the scale of individual quarries, analyses from three samples from each of the St Bees, Swinton, and Peakmoor quarries were plotted and compared (Figure 13).

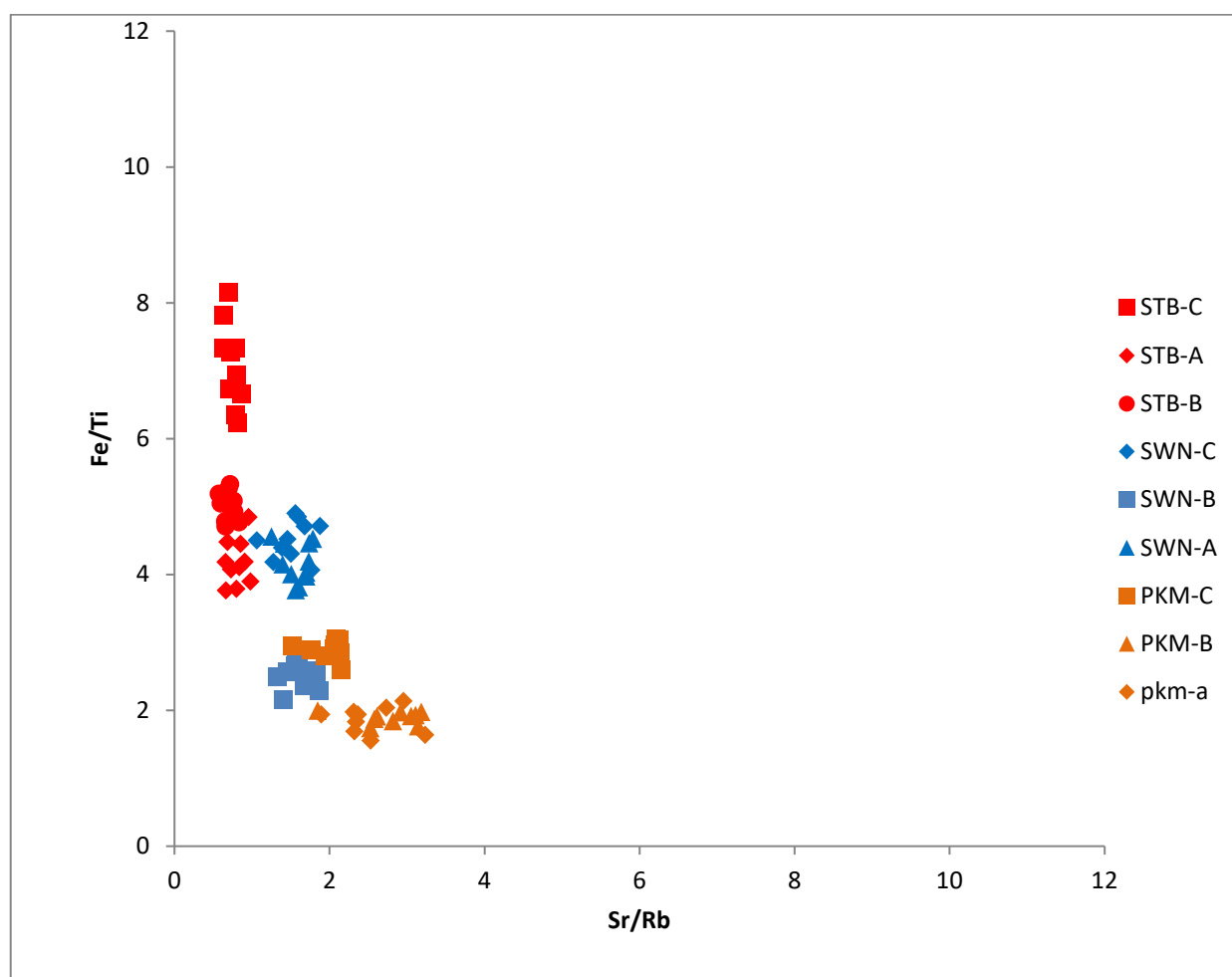


Figure 13 Plotted results of analyses of multiple samples from the same quarry

Label prefixes indicate the quarry: BLX; Blaxter, STB; St Bees, SWN; Swinton, PKM; Peakmoor. Label suffixes indicate the sample: A, B, C (see Appendix 1).

In each case, analyses derived from two of the three samples from the same quarry overlap to a significant extent while those from the third sample fall elsewhere in the plot (Figure 13). Thus, in these examples, the addition of extra samples does expand the size of the field representing each quarry (not unexpectedly), thereby increasing the chance it will overlap with the field for another quarry. However, the fields representing the three quarries shown in Figure 13 are still distinguished by distinctive shapes, sizes and positions on the chart, and the degree of overlap between them is very small. Samples from two of the quarries (St Bees and Swinton) are characterised by very narrow ranges of Sr/Rb and much larger ranges of Fe/Ti, producing narrow fields with subvertical trends on Figure 13. By contrast, samples from the third quarry (Peakmoor) have similar ranges of Sr/Rb and Fe/Ti, producing a more equant field with an inclined trend. Datasets based on at least six samples will probably be needed to establish the full size, shape and position of the composition field defining any one quarry, but these results suggest that many sandstones are likely to be characterised by fields that are sufficiently distinctive to, at least, help to constrain their provenance, and in some cases will be diagnostic.

To assess whether the method can distinguish sandstones at the bedrock unit (i.e. lithostratigraphic) scale, samples from the Peakmoor and Stanton Moor quarries, both lying within the outcrop of the Ashover Grit (Millstone Grit Group), and samples from the Crosland Hill quarry, lying within the Millstone Grit Group's Rossendale Formation, were plotted together (Figure 14).

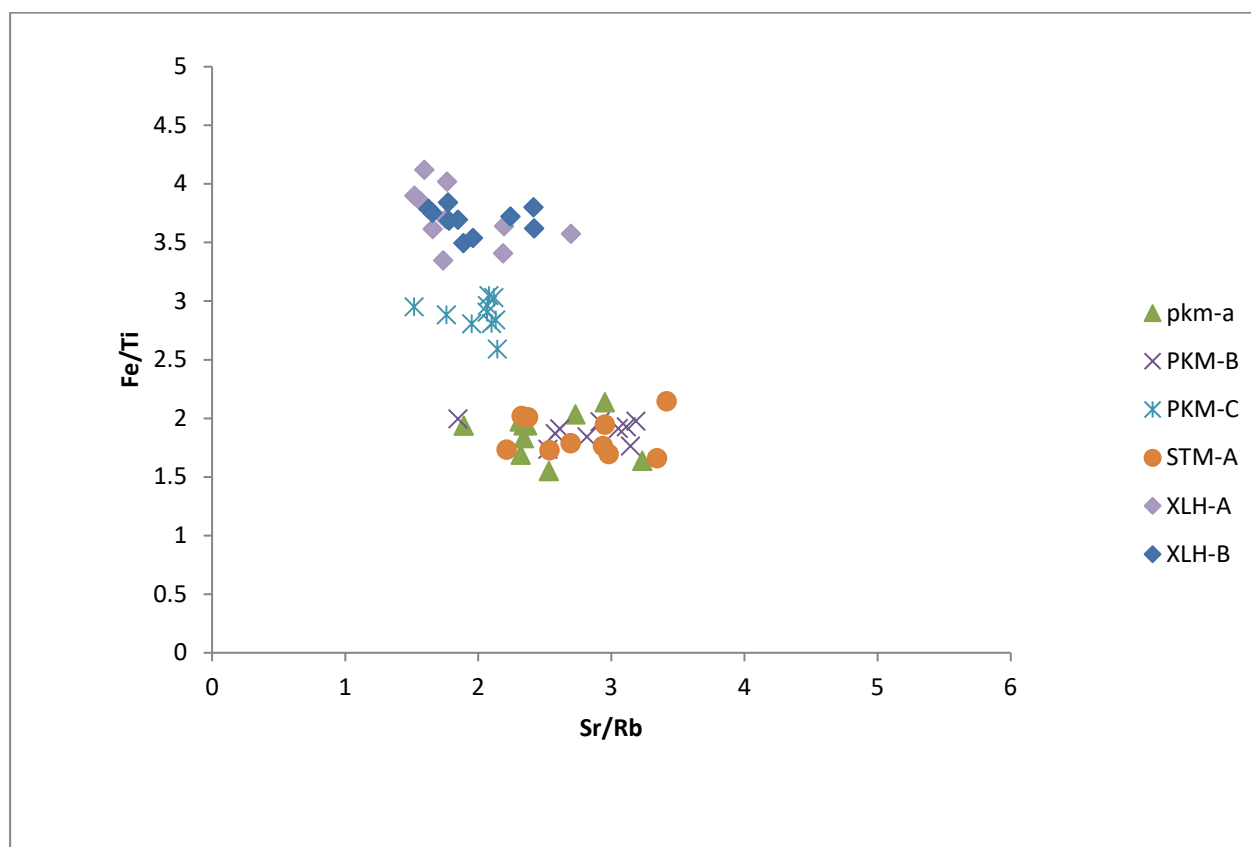


Figure 14 Plotted results for three visually similar buff sandstones

Label prefixes indicate the quarry: PKM; Peakmoor, STM; Stanton Moor; XLH; Crosland Hill. Label suffixes indicate the sample: A, B, C (see Appendix 1).

Analyses of stone from the Peakmoor and Stanton Moor quarries overlap to a large extent on the Sr/Rb vs Fe/Ti plot, whereas stone from Crosland Hill quarry is clearly distinguished by higher Fe/Ti (Figure 14). Thus, in this example at least, the method demonstrates that stone from different quarries in the same formation is closely similar, but stone from different formations within the

same group is compositionally distinct. It should be noted that stone from the Peakmoor and Stanton Moor quarries is distinguished by Ca concentration (not plotted), this being consistently above LLD in Stanton Moor samples but below LLD in Peakmoor samples.

Can the method reliably distinguish sandstones that cannot be distinguished visually?

To examine whether the method can reliably distinguish sandstones that cannot readily be distinguished visually, analyses of samples from the following groups of visually similar stones were compared:

- samples of buff sandstone from the Crosland Hill, Stanton Moor, and Peakmoor quarries
- samples of orange sandstone from Corsehill, St Bees, and Cove quarries
- samples of white sandstone from Cullalo and Craigleith quarries.

The visual appearance of these groups of sandstones is shown in Figure 15.

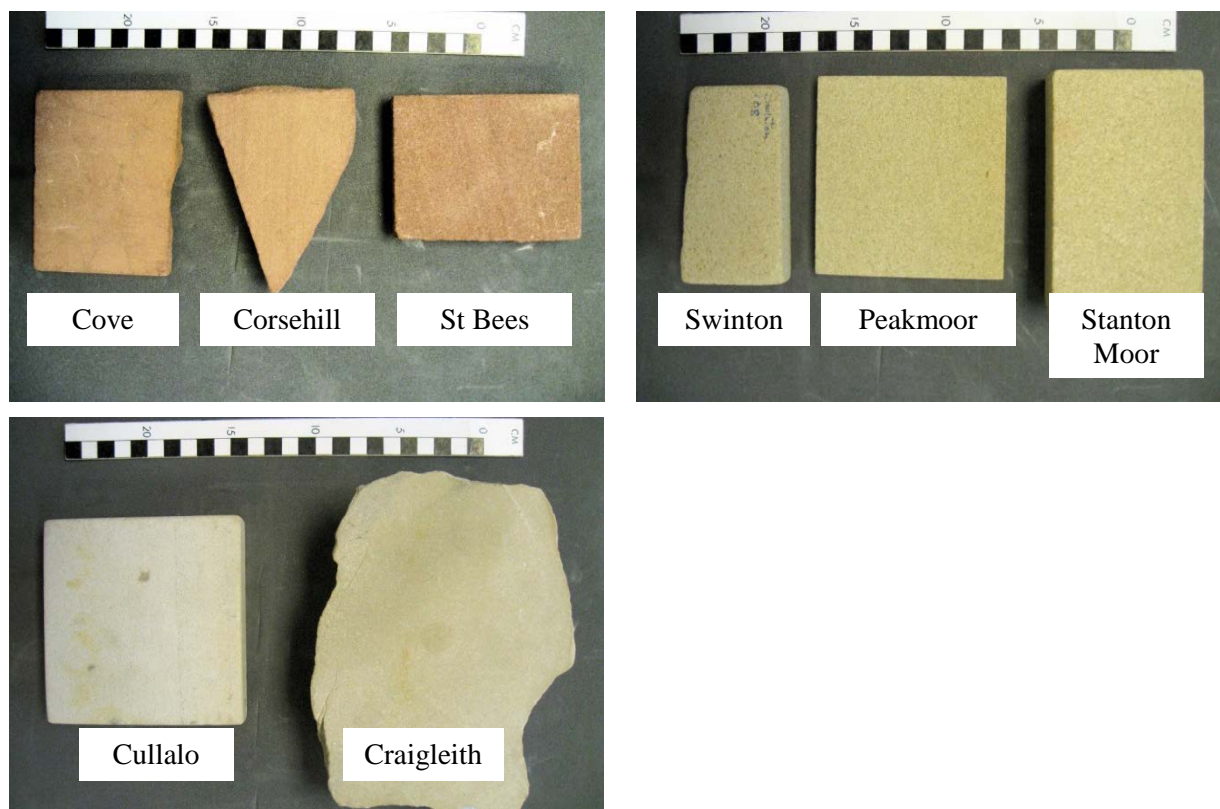


Figure 15 Photographs of visually similar sandstones selected for testing

a – orange sandstones. b – buff sandstones. c – white sandstones

Plotted results are shown in figures 14 and 16. The key findings are as follows:

- Of the three visually similar orange sandstones (Figure 15a), stone from the St Bees and Cove quarries is not distinguished on the Sr/Rb vs Fe/Ti plot (or by any other of the parameters measured by the HH-XRF instrument), whereas stone from Corsehill quarry is distinguished by slightly higher Sr/Rb (Figure 16). Although they are visually similar, and are not distinguished by the plotting parameters used here, stone from the St Bees and Cove quarries has subtly different textural features and can be distinguished visually by an experienced petrologist.
- Of the three visually similar buff sandstones (Figure 15b), stone from the Peakmoor and Stanton Moor quarries is not distinguished (i.e. occupies the same position) on the Sr/Rb vs Fe/Ti plot, whereas stone from Crosland Hill quarry is clearly distinguished by higher Fe/Ti (Figure 14). However, stone from the Peakmoor and Stanton Moor quarries is distinguished by Ca concentration (not plotted), this being consistently above LLD in Stanton Moor samples but below LLD in Peakmoor samples.
- Rb is commonly below LLD in samples of white sandstone from the Craigleith and Cullalo quarries, so the plotting parameters used here are not suitable for comparing or distinguishing these very mature sandstones. However, whereas Sr is below LLD in all analysed samples from Craigleith quarry, it is consistently above LLD in samples from Cullalo quarry. Similarly, V is below LLD in all samples from Craigleith quarry, but is consistently above LLD in samples from Cullalo quarry. Thus, HH-XRF derived data provide a useful means of distinguishing at least some very mature sandstones.

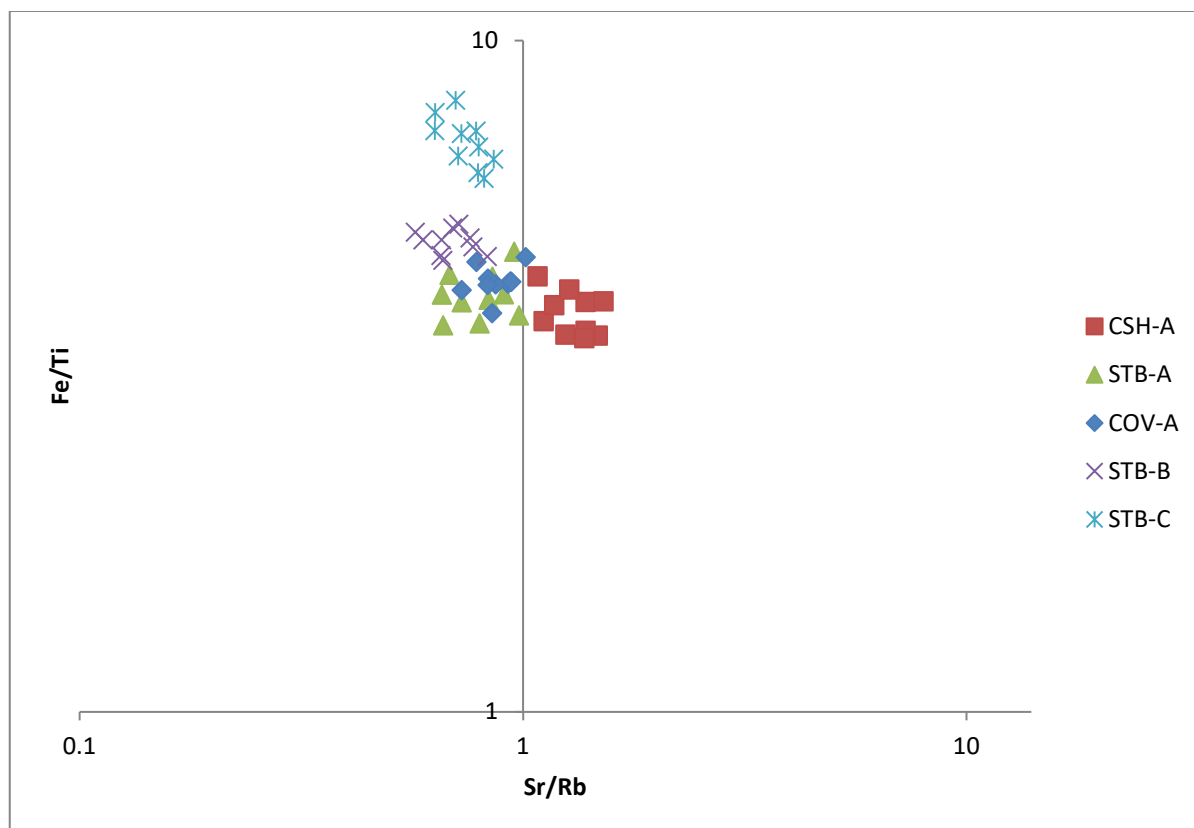


Figure 16 Plotted results for three visually similar orange sandstones

Label prefixes indicate the quarry: CSH; Corsehill, STB; St Bees; COV; Cove. Label suffixes indicate the sample: A, B, C (see Appendix 1).

5 Discussion and conclusions

5.1 EVALUATION OF EXPERIMENTAL OUTCOMES

This study has developed and tested a method for testing building stones using HH-XRF that should be robust and fit-for-purpose. The tests undertaken suggest the following methodology should be used.

- Each sample should be analysed 10 times, in order to encapsulate the inherent compositional variability of the stone at the hand sample-scale.
- The acquisition time for each analysis (with the instrument used here) should be 30 seconds; this length of time provides adequate signal for the instrument, without being too taxing for the instrument operator.
- Ideally, tests should be made on dry, flat stone surfaces. However, results obtained from rough and wetted surfaces are not significantly different.
- Plots of Sr/Rb vs Fe/Ti provide the most effective means of displaying and comparing analytical results, given that these elements are the ones most consistently above the lower limit of detection (LLD) in the analysed samples, and that these two ratios reflect different mineral combinations that form as a consequence of primary (deposition) and secondary (alteration) processes in sandstones.

Tests to determine the effect of textural variation have shown that:

- Grain size does not appear to have an impact on the consistency of analyses within the typical grain size ranges of building sandstones (fine- to coarse-sand-grade).
- The presence of bedding and lamination does not appear to influence results on the millimetre to metre scale in the tested samples. This conclusion is based on a relatively small set of samples, and the wide range of possible bedding characteristics in sandstone building stones has not been fully taken into account.

In most of the cases tested here, the method was able to distinguish between sandstones from different quarries in the same geological formation, and between sandstones that cannot be distinguished by eye. However, sandstones that are compositionally ‘very mature’ (i.e. quartz-rich), and some that are classed here as ‘mature’, tend to have very low concentrations (often below LLD) of many elements, including those used in the Sr/Rb vs Fe/Ti plots, and therefore cannot be characterised and compared using these parameters. This means that in some cases other elements in the dataset will need to be assessed to see if their concentrations or ratios are distinctive or diagnostic of individual sandstones. For example, the very mature sandstones tested here could generally be distinguished from each other by at least one of the elements detected by the instrument (e.g. Ca and V). The LLD threshold for all elements is likely to diminish as manufacturers produce more sensitive instruments.

Despite some limitations, the method devised during this study clearly has the potential to help constrain the provenance of sandstone samples and sandstone used in buildings, but a reference dataset of values for sandstones from known sources would first need to be obtained. Combining the HH-XRF ‘fingerprint’ for a sandstone with one or more other discriminatory features (e.g. a distinctive mineral or textural property) could significantly increase the capacity of the method to constrain the provenance of sandstones.

The methodology outlined in this study should also be appropriate for testing other common natural stone building materials such as mudstone/flagstone and slate using HH-XRF. The textural properties of these lithologies (fine grain size, relative homogeneity, and low or zero porosity) should be more favourable for achieving accurate and precise analytical results than those of sandstone.

5.2 POTENTIAL APPLICATIONS

The outcomes of this experimental study have shown that the portable HH-XRF instrument could have a number of building stone applications.

As described above, the main factors that currently limit the effectiveness of HH-XRF analysis of sandstone are the small number of elements that are reliably reported (consistently above LLD) by the instrument, and the inherent range of compositional variability shown by different samples from the same sandstone. This means that achieving the goal of establishing a unique geochemical signature for different sandstones will be challenging, given the huge number of quarries that have provided building stone in the past. However, the tests have shown that meaningful distinctions can be made between visually and petrographically similar stones, and that subtle differences in stone composition, textural and surface characteristics can cause a noticeable difference in results. Therefore, a well-controlled study with a clear hypothesis to test may be successful.

For example, it may be possible to identify the provenance of a sample if other background information allows the number of possible sources to be restricted. Usually, something is known about a sandstone building, such as its date of construction, location, and general character of the stone, and these may help narrow down the number of possible sources to be compared to the building sample.

An example of an application where HH-XRF testing could usefully accompany this type of approach is in identifying the source of recent stone repairs to an historic building. Since the mid C20th, there have been relatively few active building stone quarries, and the market demand tends to be for a consistent product; thus, stone quarried during the last few decades is likely to be compositionally consistent and should provide relatively consistent test results across many samples. Thus, analyses of a replacement stone of unknown origin may need only be compared with a relatively small number of different stones from active or recently active quarries. Applying HH-XRF testing to this problem could be particularly useful in ensuring conservators or contractors don't place multiple different building stones in a building, if multiple stages of repair are required.

In short, the method should be well suited to the following applications.

- Surveys of the building stones in individual buildings or settlements.
- Informing sample collection strategies for building stone surveys.
- Complementing geological observations made at a quarry, to inform a sampling strategy or in assessing compositional variability.
- Geochemical examination of weathering processes in masonry.
- Logging and comparing sandstone successions in cores and exposures.

In all these example applications, the key advantages that the method offers are speed of data collection and non-destructive testing. Test data are also objective, unlike traditional petrography and visual assessment methods which, while effective, are inherently prone to subjectivity.

Even where non-destructive methods are not essential, HH-XRF could be used to put petrography in a wider context: a thin section represents a c. 2–3 cm² area of a sample, but in some cases, interpretations made from one thin section are extrapolated to a whole building, and sometimes a whole quarry. Using HH-XRF, a large number of analyses (i.e. compositional observations) can be scattered across a sample of any scale. The data can be collected quickly and without incurring the expense of producing multiple thin sections. This could help to detect, and allow interpretation of, compositional variations and relationships between different beds of a quarry, of masonry blocks in a building, or of a group of related buildings such as a historic tenement development.

5.3 FURTHER WORK

This study has concentrated on sandstones that are visually uniform on the hand sample-scale. However, sandstones can be heterogeneous at a range of scales (e.g. due to lamination, bedding and facies variations), and further work will be needed to understand how best to deal with this.

Since exposed stone in buildings will often have undergone weathering, further work will also be needed to examine what effect different types of weathering can have on HH-XRF results, and in particular, which elements are most/least affected by weathering.

Background information should greatly enhance the ability of an HH-XRF based provenance study to make firm conclusions; the ideal application might involve a ‘decision tree’ combining some simple visual observations with geochemical criteria to constrain the source of an unknown sandstone. This could be combined with results from other non-destructive handheld applications such as infra-red spectroscopy, to provide additional data for characterisation.

The Thermo-Niton Xlt700 model used in this study was introduced in 2002. Modern HH-XRF analysers, such as the Bruker Tracer IV (launched in 2012), are not only likely to be more accurate, but they can also measure abundances of lighter elements such as Mg and Al, which are major elements in sandstones. The addition of these elements to the “toolbox” would greatly increase the available data with which to discriminate and relate analyses of sandstone samples. If a “modern” HH-XRF device is trialled for these purposes, further work should first focus on establishing whether it can reliably report concentrations of these elements.

The accuracy of the instrument when testing sandstones could be better understood by comparing HH-XRF results from a sandstone sample with high-precision laboratory-based XRF results from the same sample. In time, introducing a calibration routine that involves one or more suitable reference materials could lead to more consistent results, and a situation where results from different projects can be compared.

A large experimental error associated with the concentration values for each element is reported by the instrument. Future work to better evaluate the sources and extent of such error would be useful. The mathematical de-convolution and computation of element abundances from the raw spectra measured by the detector likely contribute significantly to the magnitude of the experimental error. It would therefore be useful to assess whether the raw spectra measured by the instrument would offer a more accurate/precise and useful “geochemical signature” than the computationally derived element concentration values. This could improve the consistency of the data, as an approach that uses parameters derived directly from the spectra would negate the additional inaccuracy introduced by the computational procedure. Since most of the potential applications of HH-XRF to building stone studies would primarily use a comparative approach, this should be appropriate, and could work well. The broad aims of such studies will be to gather quality data which can be compared to discriminate stone samples; deriving absolute concentration values for specific elements does not have to be a priority for this purpose.

6 References

- Cecil, L.G., Moriarty, M.D., Speakman, R.J. and Glascock, M.D. 2007. Feasibility of field-portable XRF to identify obsidian sources in Central Peten, Guatemala. In: Glascock, M.D., Speakman, R.J. and Popelka-Filcoff, R.S. (editors). *Archaeological Chemistry: Analytical Methods and Archaeological Interpretation* 506–521. Washington, DC: ACS Publication Series 968, American Chemical Society.
- Dyrdahl and Speakman 2013. Investigating Obsidian Procurement at Integration Period (ca. AD 700-1500) Tola Sites in Highland Northern Ecuador via Portable X-ray Fluorescence (pXRF). [Archaeological Chemistry VIII](#). Chapter 12, pp 211–232.
- Fisher, L., Gazley, M.F., Baensch, A., Barnes, S.J., Cleverly, J. and Duclaux, G., 2014. Resolution of geochemical and lithostratigraphic complexity: a workflow for application of portable X-ray fluorescence to mineral exploration [online]. *Geochemistry: Exploration, Environment, Analysis*. Available from: < <http://dx.doi.org/10.1144/geochem2012-158>>
- Historic Scotland 2012. Focus Magazine. Published by the Conservation Directorate of Historic Scotland, Edinburgh.
- Morgenstein, M., and Redmount, C. 2005. Using portable energy dispersive X-ray fluorescence (EDXRF) analysis for on-site study of ceramic sherds at El Hiba, Egypt. *Journal of Archaeological Sciences*, 32, 1613–1623.

Appendix 1: Details of samples, analyses and tests

Table 4 (overleaf) presents details of the stone samples that were tested, the analyses performed on each sample, and the scheme of alphanumeric codes that was used to label the analytical data. These codes are used in the spreadsheet of supplementary data that accompanies this report, which contains the full analytical dataset for the study.

In many cases, a set of analyses from one sample was applied during more than one stage of testing. In Table 5, details are provided of the analyses used during each stage of testing.

Table 4. Details of samples and analyses

Unless otherwise specified, all analyses were made on sawn, flat sample surfaces.

Sandstone	Sample label	BGS sample number	Analysis code	Repeat analyses	Details
Blaxter	Blaxter A	MC10297	BLX-A	x10	-
	Blaxter B	MC7333	BLX-B	x10	-
	Blaxter C	ED10488	BLX-C	x10	-
	Blaxter D	ED10815	BLX-D-ref1 BLX-D-ref2 BLX-D-Xband BLX-D-Xbed	x12 x12 x12 x12	large block; ref point 1 large block; ref point 2 large block; traverse across iron banding large block; traverse across bedding
Corsehill	Corsehill A	MC5857	CSH-A CSH-Ab CSH-Awet	x10 x10 x10	- broken surface wet surface
Cove	Cove A	MC8527	COV-A	x10	-
Craigleith	Craigleith A	MC5705	CGL-A	x19	-
Crosland Hill	Crosland Hill A	MC8535	XLH-A	x10	"fine" variety
	Crosland Hill B	MC9559	XLH-B	x10	"coarse" variety
Cullalo	Cullalo A	MC8233	CLL-A	x10	-
Peakmoor	Peakmoor A	MC8528	PKM-A PKM-Awet	x20 x10	"medium" variety "medium" variety; wet surface
	Peakmoor B	ED10806	PKM-B	x10	"coarse" variety
	Peakmoor C	MC12093	PKM-C	x10	"fine" variety
Pennant	Pennant A	MC8372 - 4	PEN-A	x20	-
			PEN-Ab	x10	broken surface
			PEN-Awet	x10	wet surface
Pitairlie	Pitairlie A (sandstone)	MC11363	PIT-A PIT-Ab	x10 x10	- broken surface
	Pitairlie B (siltstone)	MC8685	PIT-B-norm	x10	surface normal to bedding
			PIT-B-par	x10	surface parallel to bedding
Pitairlie C (siltstone)	MC11361	PIT-C-norm PIT-C-par	x10 x10	surface normal to bedding surface parallel to bedding	
St Bees	St Bees A	ED110476	STB-A	x10	"medium" variety
			STB-Ab	x10	"medium" variety; broken surface (man-made fracture)
			STB-Ab2	x10	"medium" grained variety; broken surface (natural fracture)
St Bees B	MC13070	STB-B	x10	"coarse" variety	
St Bees C	ED10972	STB-C	x10	"fine" variety	
Stanton Moor	Stanton Moor A	MC8760	STM-A	x10	-
			STM-Ab	x10	broken surface
Swinton	Swinton A	MC8228	SWN-A	x10	-
		MC8228	SWN-Ab	x10	broken surface
	Swinton B Swinton C	ED10475 ED10591	SWN-B SWN-C	x10 x10	- -

Table 5. Analyses taken into consideration during each stage of testing

Stage	Test	Analysis code	Number of analyses
1	Plotting parameters and analyses per sample	PKM-A PEN-A CGL-A	x20 x20 x19
2	Surface condition - rough vs flat	PEN-A PEN-Ab CSH-A CSH-Ab STM-A STM-Ab SWN-A SWN-Ab STB-A STB-Ab STB-Ab2 PIT-A PIT-Ab	x10 (first 10) x10 x10 x10 x10 x10 x10 x10 x10 x10 x10 x10 x10 x10
	Surface condition - wet vs dry	PKM-A PKM-Awet PEN-A PEN-Awet CSH-A CSH-Awet	x10 (first 10) x10 x10 (first 10) x10 x10 x10
3	Composition	CGL-A CLL-A BLX-A BLX-B BLX-C PKM-A PKM-B PKM-C STM-A XLH-A XLH-B CSH-A COV-A STB-A STB-B STB-C SWN-A SWN-B SWN-C PEN-A PIT-A	x10 (first 10) x10 x10 x10 x10 x10 (first 10) x10 x10 x10 x10 x10 x10 x10 x10 x10 x10 x10 x10 x10 x10 x10 x10 (first 10) x10

Stage	Test	Analysis code	Number of analyses
4	Grain size	PKM-B	x10
		PKM-C	x10
		STB-A	x10
		STB-B	x10
		STB-C	x10
		XLH-A	x10
		XLH-B	x10
	Thin bedding	PIT-B-norm	x10
		PIT-B-par	x10
		PIT-C-norm	x10
PIT-C-par		x10	
Bedding and liesegang bands in Blaxter block	BLX-D-ref1	x12	
	BLX-D-ref2	x12	
	BLX-D-Xband	x12	
	BLX-D-Xbed	x12	
5	Multiple samples	STB-A	x10
		STB-B	x10
		STB-C	x10
		SWN-A	x10
		SWN-B	x10
		SWN-C	x10
		PKM-A	x10 (first 10)
		PKM-B	x10
		PKM-C	x10
		BLX-A	x10
		BLX-B	x10
		BLX-C	x10
		Visually similar/same formation	CGL-A
	CLL-A		x10
	PKM-A		x10 (first 10)
	PKM-B		x10
	PKM-C		x10
	STM-A		x10
	XLH-A		x10
	XLH-B		x10
	SWN-A		x10
	SWN-B		x10
	SWN-C		x10
	STB-A		x10
	STB-B		x10
	STB-C		x10
	CSH-A	x10	
COV-A	x10		